STUDY OF THE FLEXURAL BEHAVIOUR OF CONCRETE BEAMS REINFORCED WITH STEEL PLATES

By

ASIT N. BAXI

B.E., M. S. University of Baroda, India, 1986

A MASTER'S THESIS

Submitted in partial fulfillment of the
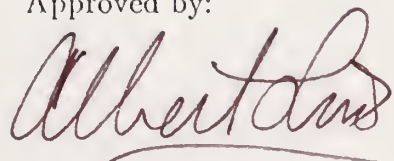requirements for the degree

MASTER OF SCIENCE

Department of Civil Engineering

KANSAS STATE UNIVERSITY

Manhattan, Kansas

1989

Approved by:

Major Professor

Contents

List of Tables

List of Figures

Chapter 1

INTRODUCTION

1.1   BACKGROUND

1.1.1   General

Concrete is a widely used construction material because of its many favourable properties. Some of these properties are: (a) its high strength-to-cost ratio, (b) its ability to be cast into almost any shape and (c) its high resistance to fire and penetration of water. However, its disadvantages are that it is a brittle material and it has a low tensile strength compared to its compressive strength. The low tensile strength of concrete is generally offset by providing suitable reinforcement capable of resisting the tension forces.

1.1.2   Types of Construction

Concrete combines with steel to result in the following three types of construction :

1. Reinforced Concrete Construction,

2. Prestressed Concrete Construction and

3. Composite or Mixed Steel-Concrete Construction.

In reinforced concrete construction, nonprestressed steel reinforcement in the form of plain or deformed reinforcing steel bars interacts with the concrete. Concrete resists the compression forces and the reinforcing steel bars resist the tension forces. Concrete in the tension zone, below the neutral axis, is assumed to be inactive. A strong chemical and mechanical bond enables the concrete to transfer forces to the steel. Vertical shearing forces are resisted by stirrups placed along the length of the beam.

In prestressed concrete members, the reinforcement is stressed to produce a pre-compression in the concrete, under the unloaded condition. The pre-compression greatly enhances the behaviour of the concrete in tension and increases the load carrying capacity of the member. High strength wires, strands, or bars are used.

Composite or mixed steel-concrete construction makes use of structural steel along with concrete. In a composite member, a standard or hybrid structural steel shape is integrally connected with concrete, so that the two together act as a unit [1, 2]. Composite, prestressed and reinforced concrete construction is at the member level, taking the form of isolated members, such as beams, columns, slabs and walls. Mixed steel-concrete systems [3] and subsystems involve the interaction of an assembly of members composing the system. Examples of this construction are composite frames, tubular and cold braced composite systems, composite cladding, etc.

1.1.3 Precast Construction

Concrete floor systems, both one-way and two-way, are used extensively in the construction of multi-story commercial, industrial and parking structures. Due to the repetitious nature of the construction, precasting of the structural members can provide overall economy.

Precast construction greatly reduces the formwork requirement. Formwork costs

can vary enormously and can have a considerable bearing on the economy of a particular design. A study of several conventional reinforced concrete projects has shown that formwork can account for between 25 to 75 percent of the total cost of a structure [4, 5]. Fully precast composite or reinforced concrete units can provide considerable economy. Cost of labor and construction time can also be reduced by using precast construction.

In practice, precasting of members using the above mentioned methods of construction is available for such structures. For example, precast reinforced concrete beams, precast fully prestressed or partially prestressed slabs and beams, and precast composite beams are all available. However, the scope for a simple precast unit still exists. The work here is an alternative method of reinforcement for such concrete floor systems.

1.2 PROPOSED SCHEME

An alternative method of reinforcing concrete beams is proposed. The longitudinal steel reinforcing bars of a conventionally reinforced concrete beam are replaced by mild steel plates. Vertical stirrups are replaced by vertical steel reinforcing bars welded on to the plate. The entire assembly is easy to prefabricate and is placed directly in the joist form. After casting of the concrete and stripping of the forms, the steel plate, exposed on the underside of the joist, can be used to support mechanical and electrical equipment, suspended ceilings and interior partitions. A schematic of the proposed scheme is shown in Fig. 1.1.

1.3 SCOPE OF THE STUDY

The primary aim of the research was to study the overall flexural behaviour of the proposed scheme of reinforcement. To prevent a horizontal slip or a vertical shear

Longitudinal Section   Section – XX

1) Stirrup or Stud

2) Concrete

3) Steel Plate

4) Weld connecting stud to plate
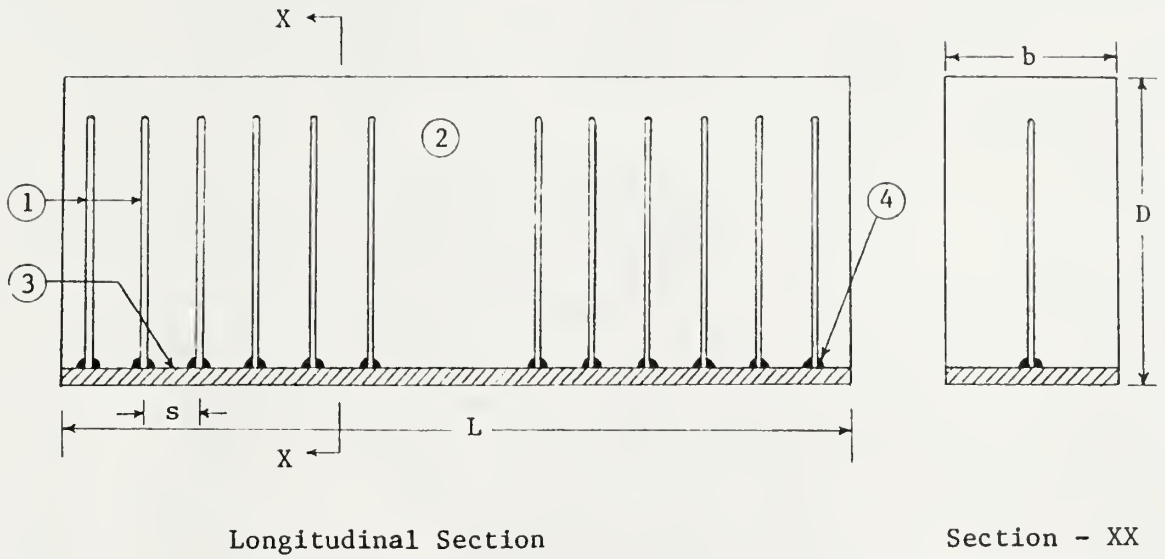
Figure 1.1: Schematic of the Proposed System of Reinforcement in Beams.

4

failure, adequate reinforcement was provided to guarantee a failure in flexure. A series of three beams, with varying steel reinforcing ratios, was tested in four point bending until failure. Load-Strain and Load-Deflection data and cracking patterns were noted. Results from the experiments were compared with results from various analyses. Conclusions were drawn regarding the overall flexural behaviour of the beams.

1.4 ORGANIZATION OF THE THESIS

The thesis is organized into six chapters. Chapter 1 introduces the proposed scheme of reinforcement. A literature review of previous work done in this area is discussed in Chapter 2. Chapter 3 discusses the theoretical background necessary for the design of the beams. Chapter 4 describes the experimental program. The experimental results, analytical results and comparisons are discussed in Chapter 5. Chapter 6 provides a summary of the work, conclusions and recommendations for further research.

Chapter 2

LITERATURE REVIEW OF PREVIOUS WORK

2.1 GENERAL

A literature review in the initial stages of the research yielded only one work [6] on the use of plates as reinforcement in concrete members. This work involved using steel plates as reinforcement in slabs. At a later stage, additional information about research in this area was obtained from several State-of-the-Art and other related reports on composite construction [3, 7, 8, 9, 10, 11]. Three more investigations, two involving plates reinforced in slabs [13, 14] and one involving beams [15], became known. Only the work done by Perry was published[16].

In the literature, plate reinforced concrete construction is also referred to as composite plate construction. Composite plates have been used for practical applications. Plates developed by Robinson [17] have been used in France for orthotropic bridge floors. Examples are the Tarcanville Suspension Bridge [17] , the Alma Bridge [18] and the Paris-Massena Cable-stayed over pass [19] near Paris.

2.2   COMPOSITE PLATE CONSTRUCTION IN SLABS

The earliest work, reported in the literature on the use of composite plates was by Casillas, Khachaturian and Siess [13] in 1957 at the University of Illinois. The purpose of their investigation was to develop design criteria for flat slabs. The objective of their tests was to determine, by means of tests on simple beams, the load-carrying capacity and behaviour of welded studs, acting as shear connectors. Two main variables were considered in their study; the stud diameter and the concrete strength. For this purpose, 12 tests were made, involving 11 beams. The tests were made using studs of three different diameters: 1/2, 5/8, and 3/4 inch. The strength of the concrete varied between 1460 psi and 5960 psi. The beams were tested under one or two concentrated loads, to obtain regions of constant shear, where the loads carried by each stud could be more easily determined. The results from these tests were used to provide design recommendations for Plate-Reinforced Flat Slabs. A photograph [13] of the plate reinforcement used is shown in Fig 2.1.

Gogoi [6] at Imperial College, London, tested seven one-way composite plates, each consisting of a 36 in. x 6 in. x 2.25 in slab connected by studs to an 1/8 in. steel plate. He also tested a two-way composite plate, 76 in. square and 2.5 in. thick supported along all four edges. It was subjected to a center point load, and failed in punching shear. The plates spanning one way only showed more slip than concrete beams due to the large tensile strain developed at the steel-concrete interface and would have required considerable shear reinforcement in practice. Two way plates were shown to have greater promise as shear forces are low except at point loads. It was concluded that elastic design methods could be used for composite plates and their shear connectors, but that propped construction would usually be necessary. The writer considered that in buildings, ultimate strength-design should lead to greater economy.
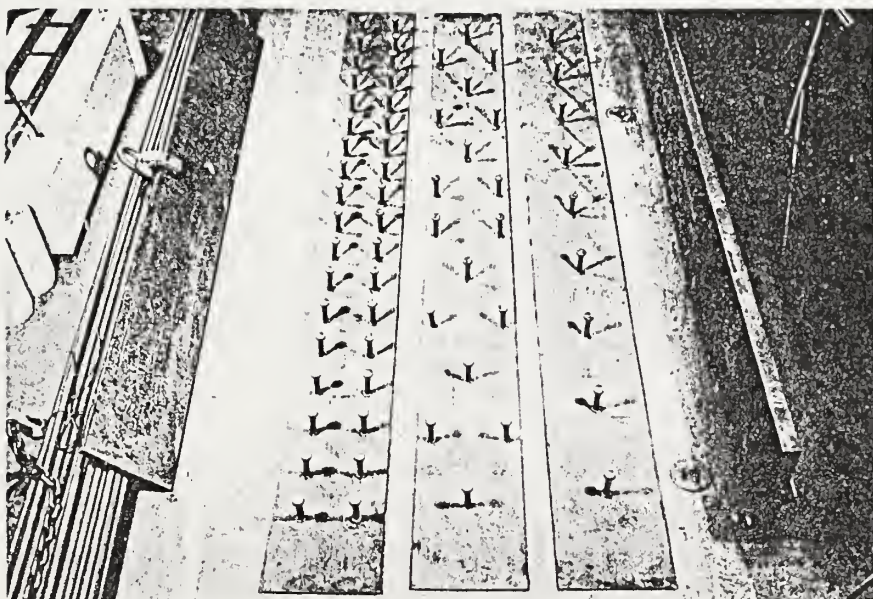
Fig. 2.1, Plate Reinforcement Assembly used by Casillas, et.al.

2.3   COMPOSITE PLATE CONSTRUCTION IN BEAMS

Perry [15], at the University of Texas at Austin, tested 26 composite beams and 14 direct shear specimens under dynamic and static loads, to determine beam behaviour and stud capacities. The main variables studied were stud diameter, concrete strength, effect of the type of loading, effect of number of studs per shear span and effect of using web reinforcement. Two types of composite beam specimens were investigated (Fig. 2.2). Beams, reinforced with a steel plate at the tension face were termed "Plate-in-tension-beams", while beams reinforced with a plate on the compression side of the concrete were termed "Plate-in-compression-beams". Perry concluded that concrete beams with steel plates, connected to the concrete by welded-stud-shear-connectors at the steel-concrete interface, behave satisfactorily as composite members under both static and dynamic loadings for slips upto 0.06 in. at the interface. Plate-in-compression beams have considerably more ductility than Plate-in-tension beams. Composite beams reinforced with steel plates may be loaded repeatedly under dynamic loadings without failure, if the loads are well within the elastic range of behaviour of the beams.

Teraszkiewicz [14] also performed tests on plate reinforced slabs and beams, but details of his work are not available.

STEEL PLATE   CONCRETE

LOAD

|6"|←— 36" —|— 36" —|6"|

12"

8"

4"

1/4"   2"

SIMPLE   SIMPLE
SUPPORT   SUPPORT

PLATE-IN-TENSION BEAM

STEEL PLATE   CONCRETE

LOAD

|6"|←— 36" —|— 36" —|6"|

1/4"

2"

8"   4"

12"

2-NO. 8 BARS

SIMPLE   SIMPLE
SUPPORT   SUPPORT   END ANCHOR PLATE

PLATE-IN-COMPRESSION BEAM
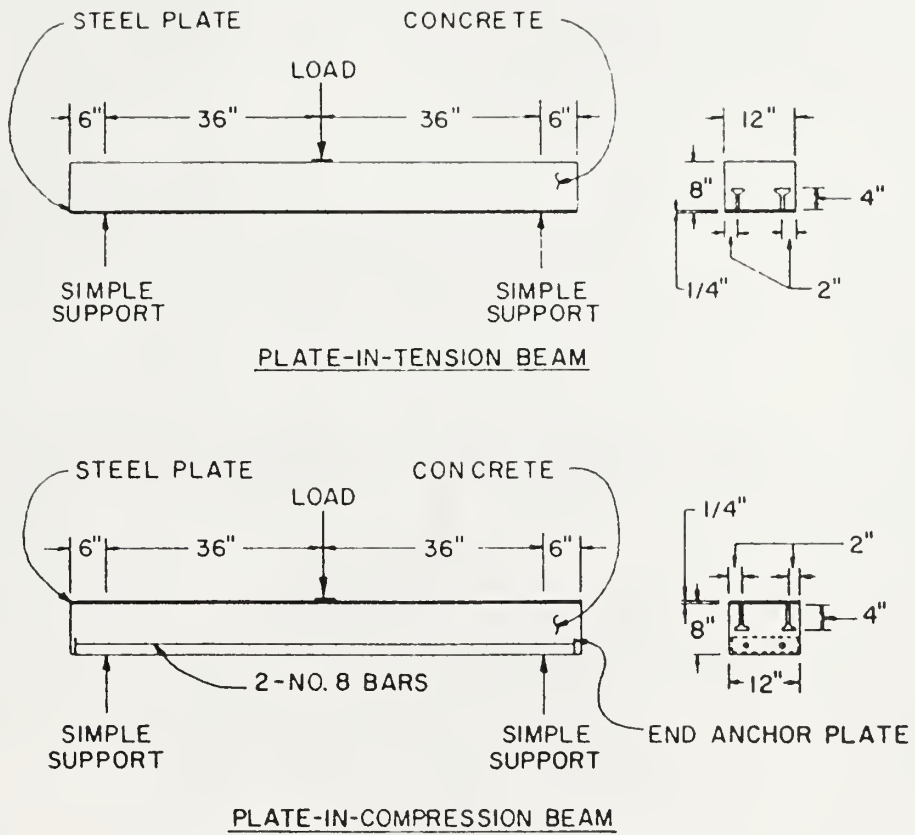
Fig 2.2, Schematic of the Composite Beam Specimens tested by Perry.

Chapter 3

THEORETICAL BACKGROUND AND DESIGN OF THE BEAMS

3.1 GENERAL

This chapter describes the theory associated with the design of the proposed scheme of reinforcement in concrete beams. The concept and general working of the scheme is explained in the following section. Section 3.3 discusses reinforced concrete behaviour in flexure and shear. Ultimate strength design and some of the current ACI Code provisions for flexural and shear design are also discussed. The fourth section discusses composite beam behaviour and the AISC specifications for allowable stress design for composite construction. Ultimate strength of composite beams and shear connectors is also discussed. The fifth section outlines the steps used for the design of the beams. The sixth and final section provides a design summary of the beams.

3.2 GENERAL WORKING OF THE SCHEME

A concrete beam using a steel plate as the tensile reinforcement is expected to behave in a similar way as a non-prestressed, singly reinforced concrete beam, reinforced with mild steel bars. At service and ultimate loads, the steel plate will resist all of the tension forces and the concrete above the neutral axis, will resist all of the compression forces. The concrete below the neutral axis is assumed to be cracked and

ineffective (ACI 10.2.5) [20]. The available natural bond in a plate reinforced beam, is limited to a chemical bond, obtained by the chemical adhesion between the steel plate and concrete above it. Since the steel plates have a smooth surface, there is no mechanical bond offered as in the case of a deformed mild steel reinforcing bar. In a deformed steel reinforcing bar, the closely spaced rib-shaped surface deformations provide a high degree of interlocking between the steel and concrete. Furthermore, the contact surface area (perimeter) for a given area of steel is lower for a plate than a fully embedded bar.

Slip at the steel and concrete interface due to horizontal shear will also occur. To provide adequate bond and prevent slip, shear connectors need to be provided. A composite action can be achieved by welding vertical bars of mild steel on the plate. The bars are welded at regular intervals along the length of the beam, between the region of zero and maximum positive moment. The function of the welded bars (stirrups) is three-fold,

1. To resist all the horizontal shearing forces,

2. To reinforce the beam for vertical shear and

3. To enable the steel plate to develop its full tension yield capacity.

The welds are designed to resist all the horizontal shear forces developed.

3.3 REINFORCED CONCRETE BEAM BEHAVIOUR

3.3.1 Behaviour in Flexure

A reinforced concrete beam, exhibits distinct stages of behaviour when it is loaded from a zero load to a load which will cause the failure of the beam.

<u>Stage 1 : Section-Elastic and Uncracked</u>

At small loads, the maximum tensile stress in the concrete is smaller than its modulus of rupture (f_r). The entire mass of concrete is effective in resisting stress, in compression on one side of the neutral axis and in tension on the other side. The reinforcement will deform the same amount as the adjacent concrete (assuming no slip), and is subject to tension stress. This represents the first stage, in which the section is elastic and the concrete has not cracked. Figures 3.1 -a,b,c illustrate the beam section at this stage and the corresponding stress distribution.

<u>Stage 2 : Section-elastic and cracked</u>

As the load is increased further, the tensile capacity of the concrete is reached and tension cracks develop. The general shape and distribution of the cracks is shown in Fig. 3.2-a. With increasing load, the cracks propagate upto or close to the level of the neutral plane, which in turn shifts upwards progressively. The presence of cracks can profoundly affect the behaviour of a beam. For example, at a section X-X in the maximum moment region where the concrete cannot resist any tension stress, the steel resists all of the tension. For moderate loads, if the concrete stresses are within a value of $f_c'/2$, the stresses and strains continue to be elastic and linearly proportional. The beam is now in its second stage where the section is elastic, but the concrete is cracked. Fig 3.2-b shows the stress-distribution at this stage.

<u>Stage 3 : Section at failure</u>

At loads, such that concrete is stressed roughly beyond $f_c'/2$, the stresses and strains are no longer linearly proportional. The ensuing non-linear relation between stresses and strains is that given by the concrete stress-strain curve shown in Fig. 3.2-c. At ultimate loads, the load carrying capacity of the beam is reached and failure occurs. Two types of flexural failure can occur, depending on the amount of the longitudinal reinforcement present in the beam. If moderate amounts of reinforcement are present, failure will occur due to the yielding of the steel in tension.
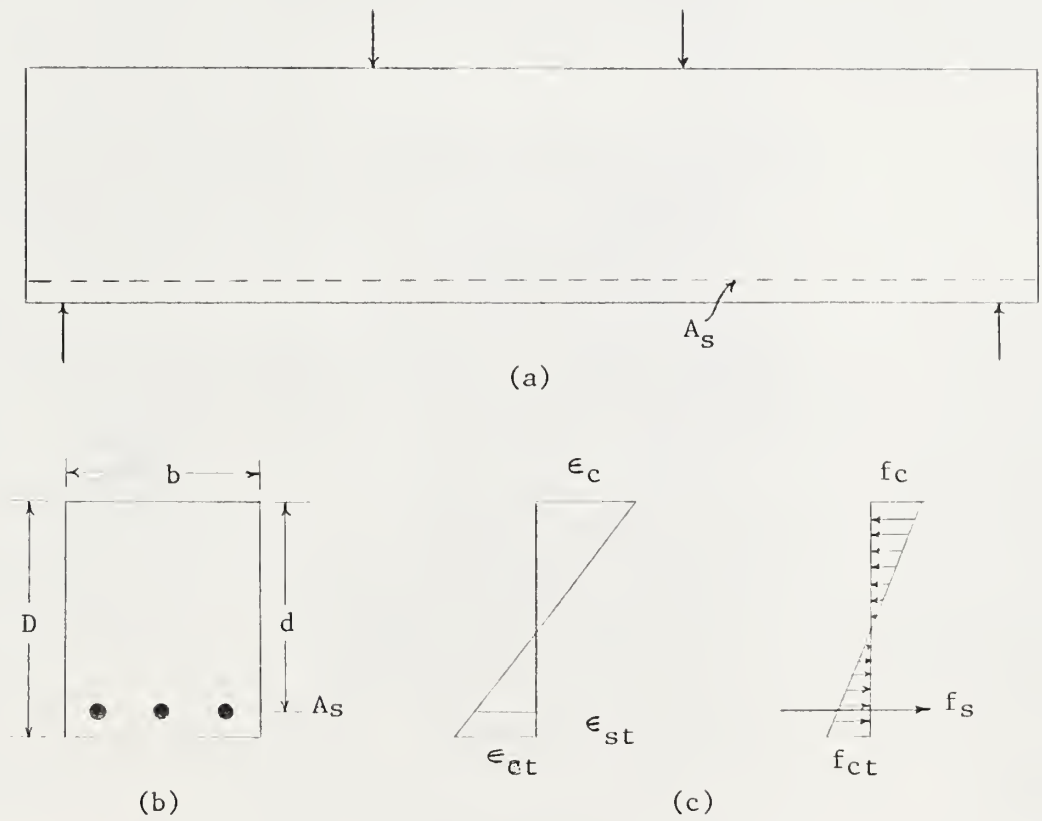
Fig 3.1, Behaviour of Reinforced Concrete Beam under Load.

14
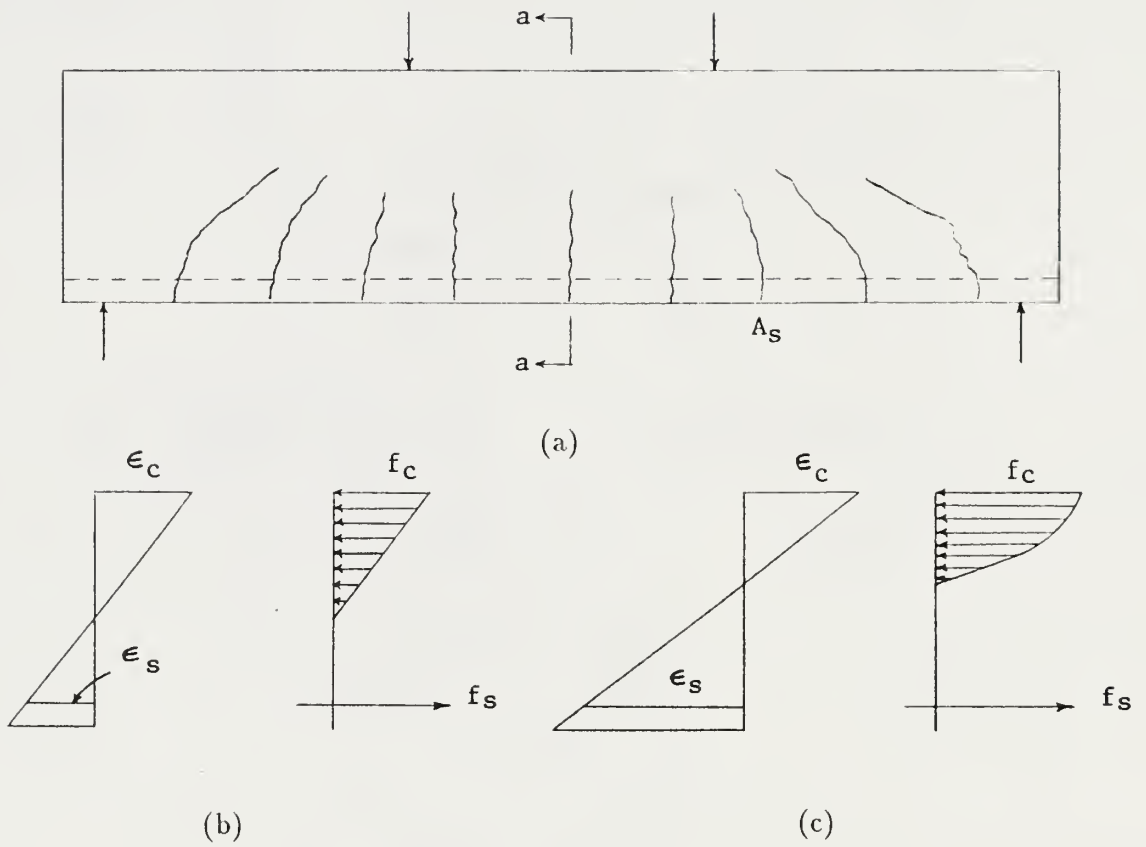
Figure 3.2: Behaviour of Reinforced Concrete Beam under Increasing Load.

On the other hand, for relatively large amounts of reinforcement, a compression failure will occur due to the sudden crushing of the concrete.

In a tension failure, the steel is first to reach its yield point, evident by a sudden stretching of the steel, visible widening of the cracks and a significant increase in deflection of the beam. When this happens, the strains in the compression zone of the concrete increase to such a degree that crushing of the concrete, the secondary compression failure, occurs. The load at this point is only slightly larger than that which caused the first yield in steel.

Concrete fails in compression, when the strains in the concrete become large enough to disrupt the integrity of the concrete. Exact criteria for this occurance are not known, but strains to the order of 0.003 to 0.004 for unconfined concrete and to 0.0065 for confined concrete [26] have been reported. The ensuing compression failure is brittle, generally explosive in nature and almost without any warning. The steel, however, may or may not have yielded depending on the resistance offered by the steel in tension. In practice and in all design codes, to account for this unpredictable behaviour of concrete in compression at ultimate loads, beams are so designed that, in case they are overloaded, a tension, and hence ductile failure should occur.

3.3.2   Ultimate Strength Design and ACI Code Provisions

3.3.2.1   Design Philosophy

Ultimate Strength or Limit State Design attempts at utilizing the ultimate capacity of a section. It differs from the philosophy of working stress design, wherein the materials exhibit only elastic behaviour and all the stresses are within specified allowable limits. Working Stress Design may yield a safer design but it is highly uneconomical.

In the case of ultimate strength design, safety factors are provided in the following two ways, by using

1. Strength Reduction Factors

2. Load Factors.

Under-strength or strength reduction factors are less than unity and denoted by ϕ. For example, the nominal moment and the nominal shear force must be modified by a factor of $\phi = 0.9$ and $\phi = 0.85$ respectively according to the ACI code. The under strength factors account for irregularities in material, construction tolerances and approximations involved in the code formulations. In general,

$$M_u \leq M_d = \phi M_n \qquad (3.1)$$

$$P_u \leq P_d = \phi P_n \qquad (3.2)$$

$$V_u \leq V_d = \phi V_n \qquad (3.3)$$

Load factors are greater than unity and are denoted by ξ. There are different values of load factors for different types of loads. For dead loads, a factor of 1.4 and for live loads, a factor of 1.7 is specified in the ACI code. There are different values of load factors for seismic, wind, and other types of loads. The overload factors are based on probabilistic and reliability considerations.

Another important consideration to be made in strength design, is serviceability requirements. Deflections should not be excessive. Cracks should be narrow in width and well distributed througout the tensile zone.

3.3.2.2 Formulation

From the previous discussion, it has been shown that stresses in the concrete are not proportional to strains, after the concrete is stressed beyond $f'_c/2$. Experiments

by other researchers have proved that the strain variation across the depth of a beam is linear even at ultimate loads. However, there is no well defined shape observed for the stress distribution in the concrete. Various stress blocks have been proposed - parabolic, rectangular, trapezoidal etc. In the United States, the rectangular stress block, first proposed by C.S. Whitney and subsequently elaborated and checked experimentally by others [25], is most commonly used. Formulation of flexure relations in the ACI Code are based on the use of this stress block. A wholly rational theory for determining the ultimate strength of reinforced concrete beams is difficult to develop. Hence, present methods are based in part on the laws of mechanics, supplemented, where needed, by extensive test information.

Equivalent Rectangular Stress Distribution (Whitney Stress Block)

The formulation of strength analysis can be greatly simplified by replacing the actual complex stress distribution (Fig 3.3) in concrete by a simple geometric shape (Fig 3.4), provided the total compression force C and its location with respect to the neutral axis is the same. The stress distribution is rectangular, and is commonly referred to as the Equivalent Rectangular Stress Distribution or simply called the Whitney Stress Block. From the figure,

$C = \alpha f'_c bc = \gamma f'_c ab$ which gives $\gamma = \frac{\alpha c}{a}$

α is defined as the ratio of the average compressive stress on the area in compression bc to the maximum compressive strength f'_c. β is the fraction of the depth of the neutral axis at which the total force C is located.

The depth of the rectangular stress distribution is defined as a and is given by $a = \beta_1 c$. This gives $\gamma = \alpha/\beta_1$ and from which follows, $\beta_1 = 2\beta$.

From experimental investigations and in the ACI Code (10.2.7.3) [20], β_1 and γ are defined as follows
$\beta_1 = 0.85 - 0.05(f'_c - 4000)/1000$ and $\beta_1 = 0.65$ for $f'_c > 8000$ psi.
$\gamma = 0.85$ for $f'_c < 7000$ psi and $\gamma = 0.86$ for $f'_c \geq 7000$ psi.
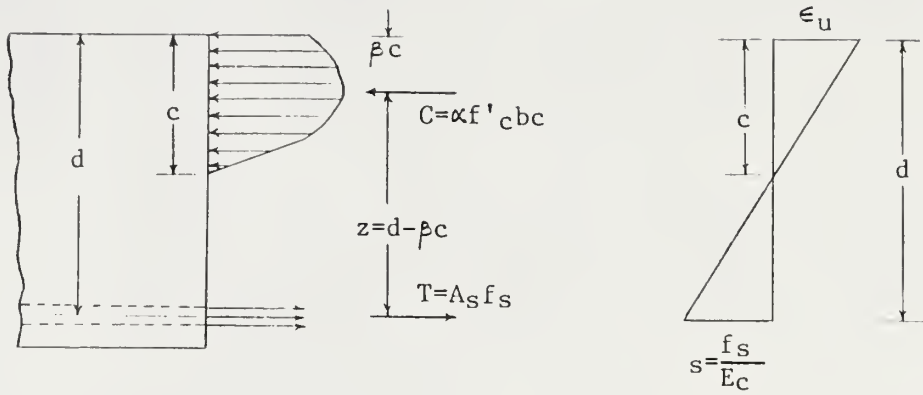
Figure 3.3: Stress Distribution at Ultimate Load.
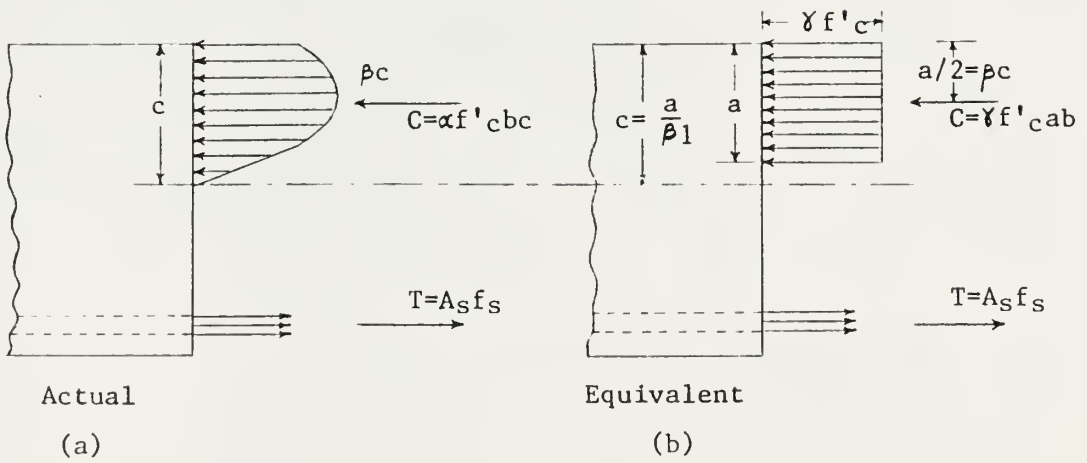
Figure 3.4: Actual and Equivalent Rectangular Stress Distribution at Ultimate Load.

19

Since, compression failure occurs explosively and without warning, in practice it is advisable to keep the amount of reinforcement sufficiently small. This ensures that, if the member is overloaded, it will give an adequate warning, before failing in a gradual manner by yielding of the steel. This is achieved by keeping the steel reinforcement ratio $\rho = A_s/bd$ below a certain value called the balanced steel ratio, ρ_b. The balanced steel ratio represents the amount of reinforcement necessary to cause the simultaneous crushing of the concrete and yielding of the steel. Hence, when $f_s = f_y$ and concrete reaches its ultimate strain ϵ_u, the steel percentage required for this condition is ρ_b. The critical position of the neutral axis (from the strain diagram, Fig. 3.5-b) for this condition is given by,

$$c = \frac{\epsilon_u}{\epsilon_u + \epsilon_y}.d \tag{3.4}$$

Compression and tension forces are given by,

$$T = \rho_b f_y bd \tag{3.5}$$

and

$$C = 0.85 f'_c ab = 0.85 f'_c \beta_1 bc \tag{3.6}$$

Applying laws of equilibrium and assuming that plane sections remain plane, $C = T$,

$$0.85 f'_c \beta_1 bc = \rho_b f_y bd \tag{3.7}$$

which gives

$$\rho_b = \frac{0.85 \beta_1 f'_c}{f_y} \frac{\epsilon_u}{\epsilon_u + \epsilon_y} \tag{3.8}$$

and substituting $\epsilon_u = 0.003$ (ACI 10.3.2) and $E_s = 29\mathrm{x}10^6$ psi (ACI 8.5.2),

$$\rho_b = \frac{0.85 \beta_1 f'_c}{f_y} \frac{87000}{87000 + f_y} \tag{3.9}$$

The maximum permissible steel reinforcing ratio in the ACI Code (10.3.3) is limited to $\frac{3}{4}\rho_b$ and the minimum (10.5.1) to $200/f_y$.
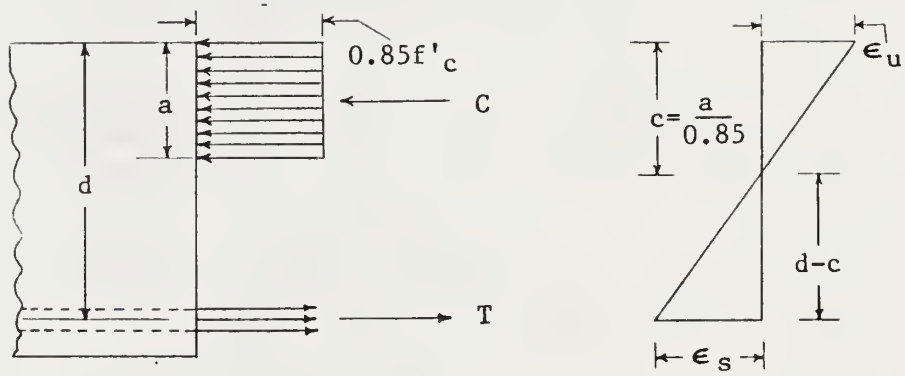
Figure 3.5: Strain and Equivalent Stress Distribution at Flexural Failure.

The nominal moment for a given steel reinforcing ratio ρ is given by,

$$M_n = \rho f_y b d^2 (1 - 0.59\rho\frac{f_y}{f'_c})$$ (3.10)

and

$$M_u = \phi M_n \qquad (\phi = 0.9)$$ (3.11)

3.3.3 Reinforced Concrete Behaviour in Shear

3.3.3.1 Diagonal Tension

Reinforced concrete beams can also fail in shear. The shear failure occurs more because of the diagonal tension failure of the concrete, rather than by the direct shearing of the concrete. The diagonal tension results from a combination of shear stress and longitudinal flexural stress. Consider a small square element, located at the neutral axis of a beam, loaded as in Fig. 3.6-a and isolated as shown in Fig. 3.6-b. The stresses acting on the element, constitute equal and opposite vertical shear stresses and corresponding horizontal shear stresses, to prevent the rotation of the element. The action of these pair of shear stresses is the same as that of two normal stresses, one tension and one compression, acting on the 45 degree faces of the element and of numerical value equal to that of the shear stresses (Fig. 3.6-c). The normal stresses are commonly known as the principal stresses. For a general case, they can be equated by the following equation,

$$t = \frac{f}{2} \pm \sqrt{\frac{f^2}{4} + v^2}$$ (3.12)

where,

f - bending stress

v - shear stress and

t - principal stress.
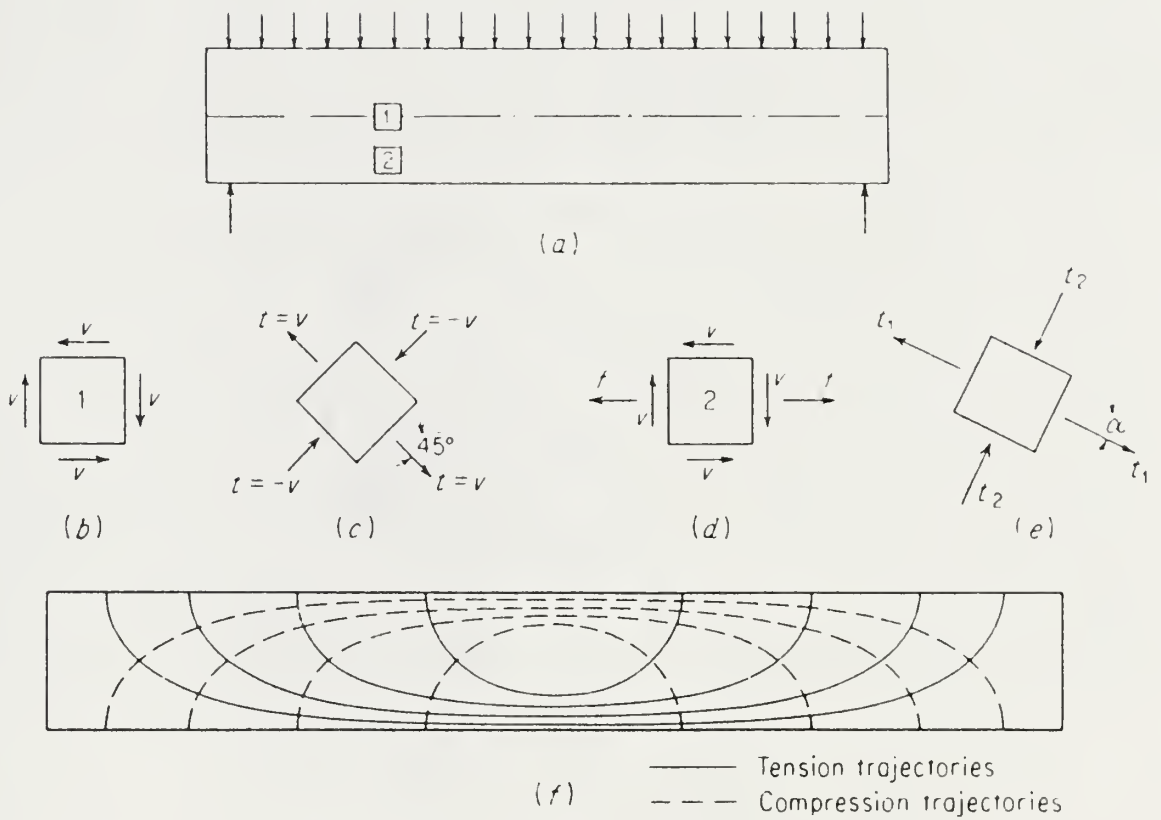
Figure 3.6: Stress Trajectories in a Homogeneous Rectangular Beam[21].

The inclination of the principal stresses can be computed from the equation $tan2\alpha = 2v/f$. The principal stresses can be computed at other locations in the beam, as in Fig. 3.6-d,e and stress trajectories plotted as in Fig. 3.6-f.

When the diagonal tension exceeds the tension capacity of the concrete, diagonal cracks occur due to the splitting of the concrete. Hence the concrete must be reinforced with suitable shear reinforcement, commonly referred to as web reinforcement.

3.3.3.2 Action of Web Reinforcement

Web reinforcement is usually in the form of vertical stirrups, spaced at regular or varying intervals along the length of the beam. The web reinforcement becomes effective mainly after the formation of diagonal cracks in the concrete. It augments the shear resistance of a beam in the following four ways:

1. A part of the shear force is resisted by the bars which intersect a particular crack.

2. The presence of these same bars restricts the growth of diagonal cracks and reduces their penetration into the compression zone. This leaves more uncracked concrete for resisting the combined action of compression and shear.

3. They counteract the widening of the cracks by the action of the interface force V_i (Fig 3.7), so that the two crack faces stay in close contact with each other.

4. They provide some measure of restraint against the splitting of concrete along the longitudinal reinforcement because of the arrangement of stirrups along the length of the beam.

Hence it can be inferred that failure is imminent when the stirrups start yielding, exhausting not only their own resistance, but permitting a wider crack opening, consequently reducing all the restraining effects mentioned above.
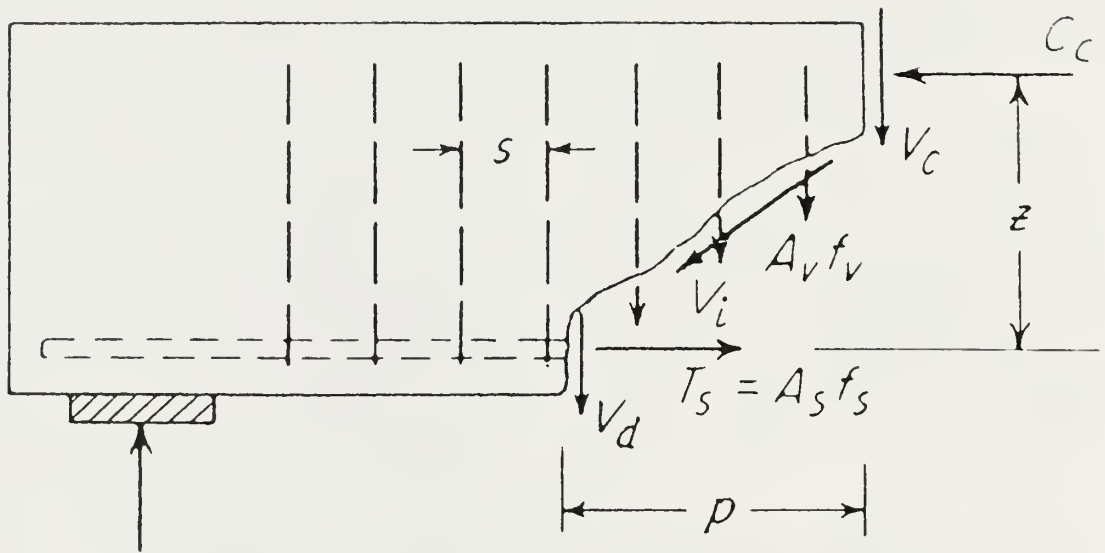
Figure 3.7: Forces at Diagonal Crack in Beam with Vertical Stirrups[21].

3.3.3.3   Formulation and ACI Code Provisions

Since web reinforcement is ineffective in the uncracked beam, the magnitude of the shear force or shear stress which causes cracking to occur is the same as would be in a beam without web reinforcement. The magnitude of this shear force, from a large number of test results [23], is given by:

$$v_{cr} = \frac{V_{cr}}{bd} = 1.9\sqrt{f'_c} + 2500\frac{\rho V d}{M} \leq 3.5\sqrt{f'_c} \qquad (3.13)$$

where,

$V_{cr} = v_{cr}.bd$ and $\rho = \frac{A_s}{bd}$

2500 is an empirical constant in psi units and

V, M are the external shear force and bending moment respectively, acting at the given section.

The various forces acting on a portion of a beam reinforced with vertical stirrups between a crack and the nearby support are shown in Fig. 3.7. V_i represents the interlock force present along the crack due to the surface roughness. This force has been measured to be sizeable, amounting to one-third or more of the total shear force. The other internal forces, are those in the uncracked portion of the concrete at the top of the beam V_{cz} and across the longitudinal steel, acting as a dowel V_d. As far as the forces exerted by the stirrups are concerned, each stirrup traversing the crack exerts a force $A_v f_v$ on the given portion of the beam. A_v is the cross-sectional area of the stirrup, twice the area of the bar, if two legged, and four times if four legged. f_v is the tension stress in the stirrup.

For equilibrium in the vertical direction,

$$V_{ext} = V_{cz} + V_d + V_{iy} + V_s \qquad (3.14)$$

where $V_s = nA_v f_v$ is the total vertical force in the stirrups, n being the number of stirrups traversing the crack. So if s is the stirrup spacing and p the horizontal projection of the crack, as shown, then $n = p/s$.

While the total shear carried by the stirrups at yielding is known, the individual magnitudes of the three other components are not known. Based on the limited amounts of test evidence, it is conservatively assumed that prior to failure of a web-reinforced beaı

$$V_c + V_d + V_{iy} = V_{cr} \tag{3.15}$$

According to the ACI Code (11.3.2.10), the value for V_{cr} is the same as Eq. (3.13) expressed in terms of stress.

The more conservative and less accurate equation in ACI (11.3.1.1) is also permitted, for simplicity in design, and is given by:

$$V_c = 2\sqrt{f'_c} b_w d \tag{3.16}$$

where
b_w - web width for T-sections or beam width for rectangular sections, in.
d - effective depth to tensile steel, in.
f'_c- specified compressive strength of concrete.

The shear to be carried by the stirrups V_s, is given by:

$$V_s = \frac{V_u}{\phi} - V_c \tag{3.17}$$

where
V_u - ultimate factored shear force at section

ϕ- strength factor for shear ($\phi = 0.85$)

The stirrup spacing can then be calculated by the equation:

$$s = \frac{A_v f_y d}{V_s} \tag{3.18}$$

where

A_v - total cross-sectional area of web steel, sq. in.

f_y - yield strength of web steel, psi or ksi.

According to ACI-(11.5.4.1), stirrup spacing is limited to a minimum of

$\frac{A_v f_y d}{V_s}$

$d/2$

or 24 in.

Also, when V_s exceeds $4\sqrt{f_c'}b_w d$, the maximum spacings of section 11.5.4.1 should be reduced by one-half. V_s shall not exceed $8\sqrt{f_c'}b_w d$.

3.4   COMPOSITE BEAM BEHAVIOUR

3.4.1   Composite Action

Composite Construction in steel and concrete refers to the use of structural steel along with concrete so that the two are integrally connected and act together as a unit. Examples of composite construction are a reinforced concrete slab on a rolled steel beam, a reinforced or an unreinforced slab on a plate, a tubular or a box column filled with concrete, etc. The extent to which composite action is developed depends on the degree to which linear strain is maintained, from the top of the concrete slab to the bottom of the steel section.

The concept of composite behaviour can be explained by considering the non-

composite beam shown in Fig. 3.8-a. The beam and slab each carry a part of the load, assuming that no frictic exists between the two. When the slab deforms under vertical load, its lower surface is in tension and elongates, while the upper surface of the beam is in compression and shortens. Thus, a discontinuity will occur at the plane of contact. When a system acts compositely (Fig.3.8-b), no relative slippage occurs between the slab and the beam. Horizontal forces (shears) are developed that act on the lowe urface of the slab to compress and shorten it, while simultaneously they act on the upper surface to elongate it.

An examination of the strain distribution that occurs when there is no interaction between the steel beam and the concrete slab (Fig. 3.9-a) shows that the steel resisting moment is equal to

$$\Sigma M = M_{slab} + M_{beam}$$

The figure shows two different neutral axes and the horizontal slippage at the steel and concrete interface. If some amount of interaction (Fig. 3.9-b) is considered, then it is observed that the neutral axes become closer to each other. The partial interaction gives rise to partial development of the compressive and tensile forces C' and T', which increase the moment capacity of the section to the amount $C'e'$ or $T'e'$. For a case of complete interaction (3.10-c), no slippage is developed at the steel and concrete interface and the strain diagram has no discontinuities. There is only one neutral axis, the compressive and tensile forces C'' and T'' are larger than C' and T' and the composite section develops its full moment capacity,

$$\Sigma M = T''e'' = C''e''$$

3.4.2 Allowable Stress Design

The allowable stress design for a composite beam is based on limiting the stress in the steel at service loads. The stress at the extreme fiber is limited to a value of $0.66\ f_y$ for wide flange sections. The section modulus of the composite section is
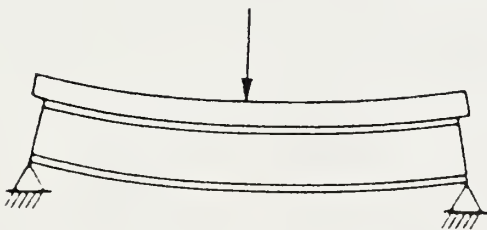
(a) Deflected noncomposite beam
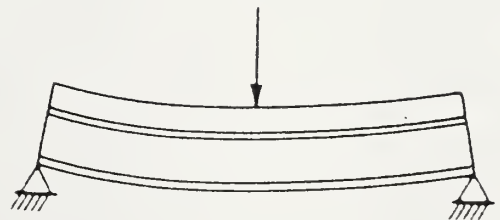
(b) Deflected composite beam

Figure 3.8: Comparison of Deflected Beams with and without Composite Action[2].
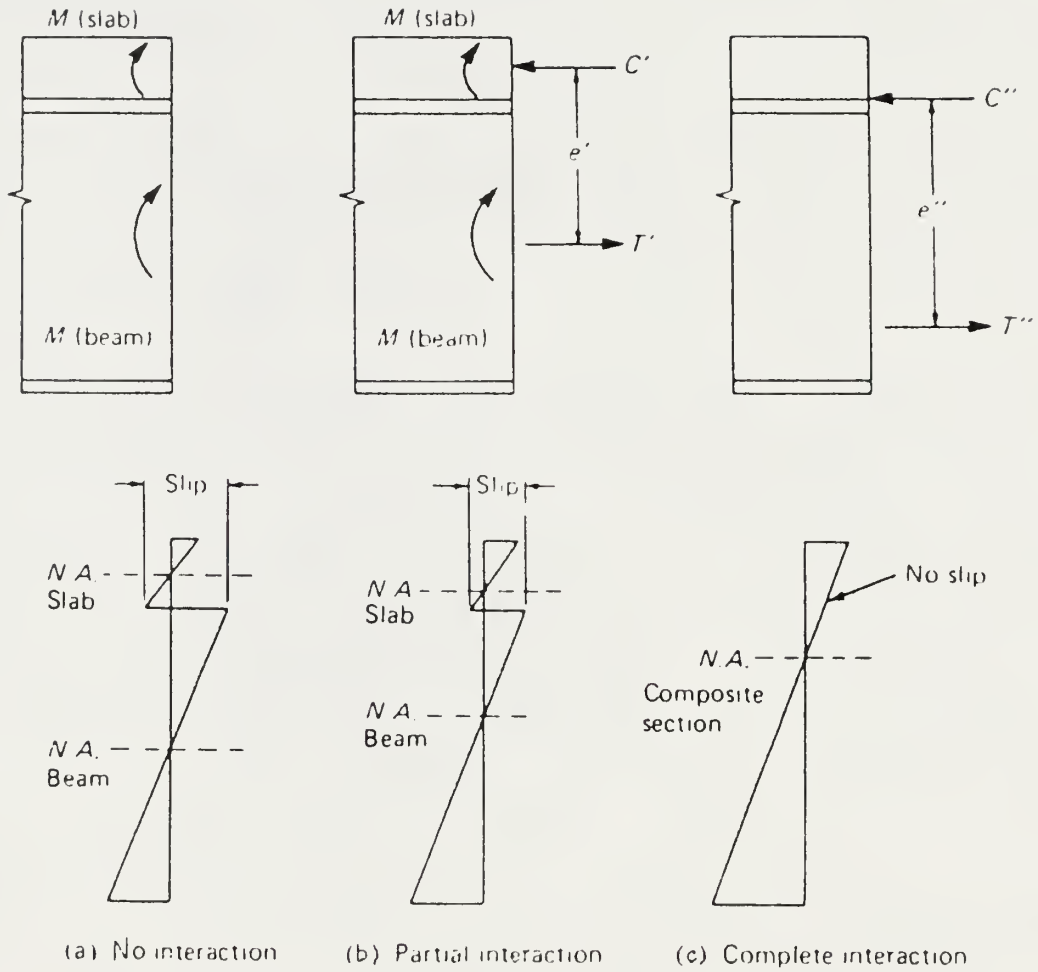
Figure 3.9: Strain Variation in Composite Beams[2].

obtained by transforming the concrete area to steel. Effects of bracing, compactness of a section and shoring requirements are considered in the design [22].

3.4.3 Ultimate Strength Design

The ultimate strength of a composite section is dependent upon the yield strength and section properties of the steel beam, the concrete slab strength, and the interaction capacity of the shear connectors joining the slab of the beam.

The provisions of AISC-1.11 [22] are nearly all based on ultimate strength behaviour, even though all relationships are adjusted to be in the service load range. These ultimate strength concepts were applied to design practice as recommended by the ASCE-ACI Joint Committee on Composite Construction [1], and further modified as result of the work of Slutter and Driscoll [24].

In determining the ultimate moment capacity, the concrete is assumed to take only compressive stress. Although concrete is able to sustain a limited amount of tensile stress, the tensile strength at the strains, occuring during the development of the ultimate moment capacity is negligible.

The procedure for determining the ultimate moment capacity depends on whether the neutral axis occurs within the concrete slab or within the steel beam. If the neutral axis occurs within the slab, the slab is said to be adequate, i.e., the slab is capable of resisting the total compressive force. If the neutral axis falls within the steel beam, the slab is considered inadequate, i.e., the slab is only able to resist a portion of the compressive force, the remainder being taken by the steel beam. Fig. 3.10-a,b shows the stress distribution for these two cases.
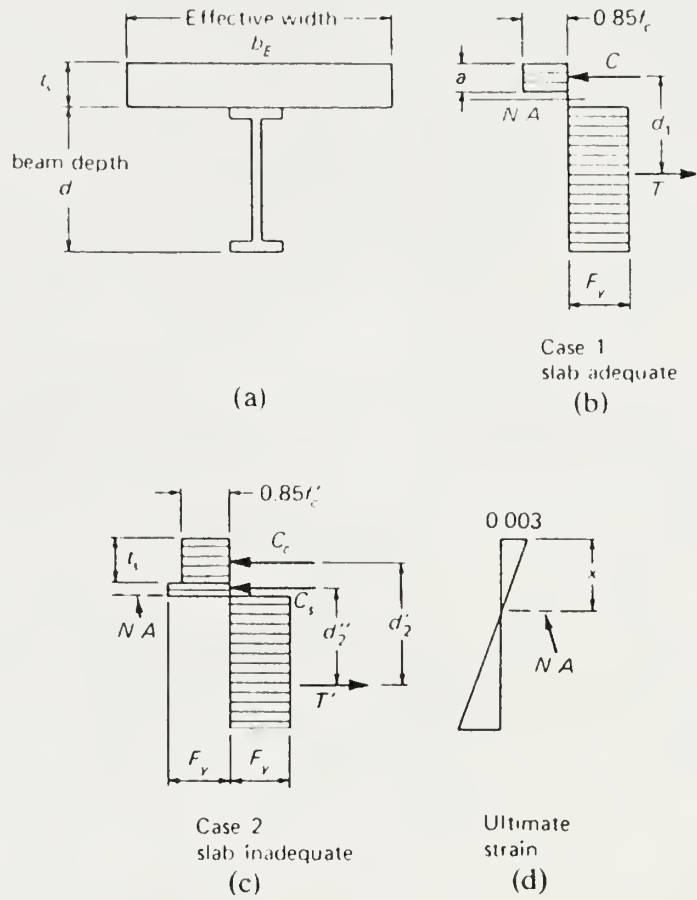
Figure 3.10: Stress Distribution at Ultimate Moment Capacity[2].

Case 1 - Slab Adequate

Assuming the Whitney rectangular stress block, the ultimate compressive force C is

$$C = 0.85 \, f_c' \, ab_E \tag{3.19}$$

The ultimate tensile force T is the yield strength of the beam times its area :

$$T = A_s f_y \tag{3.20}$$

Equating C and T,

$$a = \frac{A_s f_y}{0.85 \, f_c' b_E} \tag{3.21}$$

Ultimate Moment capacity, M_n, is then given by

$$M_n = C d_1 \, or \, T d_1 \tag{3.22}$$

Expressing the ultimate moment in terms of the steel force gives

$$M_u = A_s f_y \left(\frac{d}{2} + t_s - \frac{a}{2} \right) \tag{3.23}$$

Case 2 - Slab Inadequate

If the depth of the stress block as determined in Eq. (3.21) exceeds the slab thickness, the stress distribution will be as shown in Fig. 3.10-c. The ultimate compressive force C_c in the slab is

$$C_c = 0.85 f_c' b_E t_s \tag{3.24}$$

The compressive force in the steel beam resulting from the portion of the beam above the neutral axis is shown in the figure as C_c.

The ultimate tensile force T' which is now less than $A_s f_y$ must equal the sum of the compressive forces :

$$T' = C_c + C_s \tag{3.25}$$

Also,

$$T' = A_s f_y - C_s \tag{3.26}$$

Equating (3.25) and (3.26), C_s become

$$C_s = \frac{A_s f_y - C_c}{2} \tag{3.27}$$

$$C_s = \frac{A_s f_y - 0.85 f_c' b_E t_s}{2} \tag{3.28}$$

Considering the compressive forces C_c and C_s, the ultimate moment capacity M_u for Case 2 is,

$$M_u = C_c d_z' + C_s d_z' \tag{3.29}$$

3.4.4   Shear Connectors

The horizontal shear, that develops between the concrete slab and the steel beam during loading, must be resisted so that the composite section acts monolithically. Although, the bond developed between the slab and the steel beam may be significant, it cannot be depended upon to provide the required interaction. Neither can the frictional force between the slab and the steel beam.

Instead, mechanical shear connectors attached to the top of the beam must be provided. Shear connectors are of different types, such as stud, channel, spiral, angle connectors, etc.

Design -Ultimate Strength Concept

The connection and the beam must resist the same ultimate load. However, under service loads the beam resists dead and live loads, and unless shores are used, the connectors resist essentially, only the live load. Working stress method might design the connection only for live load, however, an increased factor is used, since the ultimate capacity would be otherwise inadequate.

35

AISC-1.11 uses an ultimate strength concept but converts both the design forces and the connector capacities into the service load range by dividing them by a factor. Thus, for design under service loads,

$$V_h = \frac{C_{max}}{2} = \frac{0.85 f'_c A_c}{2} \qquad (3.30)$$

which is AISC formula (1.11-3), and where $A_c = b_E t_s$, the effective concrete area AISC (1.11-4) is

$$V_h = \frac{T_{max}}{2} = \frac{A_s f_y}{2} \qquad (3.31)$$

where V_h -horizontal shear to be resisted between the points of maximum positive moment and points of zero moment, the smaller of Eq. (3.30) or Eq. (3.31) is used. $f'_c = 28$ day compressive strength of concrete
$A_c = b_E t_s =$ effective concrete area
$A_s =$ area of steel beam
$f_y =$ yield stress of steel

The number of connectors is obtained by dividing the smaller value of V_n by the allowable shear per connector :

$$N = \frac{smaller\ V_h}{q} \qquad (3.32)$$

3.5   DESIGN STEPS

The design of the test beams was reduced to the determination of one parameter, the stirrup spacing, since the other parameters such as the steel reinforcing ratio, width and depth of the beam were predetermined. Description of the test specimens is contained in the next chapter.

The following steps were involved in the design of the beams.

(A) Design for flexure.

1. Balanced Steel Ratio (ρ_b):

Using the same terms as described in the earlier sections,

$$\frac{c}{d} = \frac{\epsilon_u}{\epsilon_y + \epsilon_u} = \frac{0.003}{\frac{f_y}{E_y} + 0.003}$$

$$C = 0.85 f_c' b \beta_1 c$$

$$T = A_s f_y = \rho_b b d f_y$$

Equating C and T,

$$\rho_b = \frac{K}{f_y} \cdot \frac{c}{d} \tag{3.33}$$

where, $K = 0.85 f_c' \beta_1$

2. Steel Reinforcing Ratio (ρ):

$$\rho = \frac{A_s}{bd} = \frac{t}{d} \qquad (A_s = bt) \tag{3.34}$$

where, t = thickness of the plate.

3. Moment Capacity of the Beams (M_u) :

$$M_u = \phi \rho f_y b d^2 (1 - \frac{0.59 \rho f_y}{f_c'}) \tag{3.35}$$
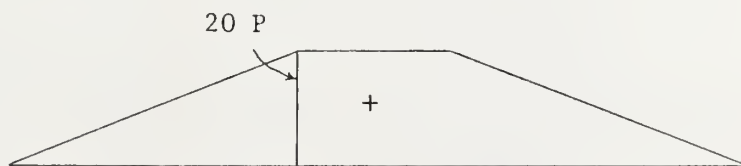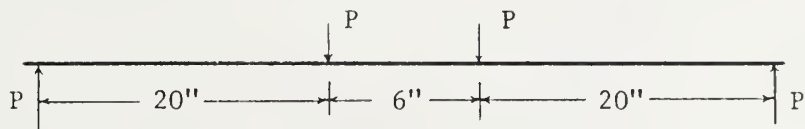
(B) Design for Shear.

Vertical Shear

1. Ultimate Shear Load Acting on the Beam (V_u):

Based on a four point bending scheme, as shown in Fig. 3.11,

$$P_u = \frac{M_u}{20} \tag{3.36}$$

and V_u at 'd' from the support $= P_u$

P   P

P |——— 20" ———|—— 6" ——|——— 20" ———| P

20 P

+

Moment Diagram

P   +

—   P
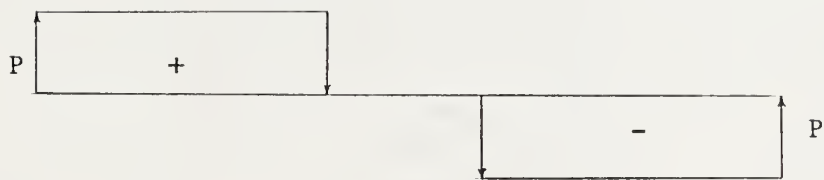
Shear Diagram

Figure 3.11: Four Point Loading Scheme.

where

M_u = Ultimate Moment in in-kips

V_u = Ultimate Shear load in kips

2. Shear to be carried by the stirrups (V_s):

$$V_c = 2\sqrt{f_c'}bd \qquad ; \qquad V_s = \frac{V_u}{\phi} - V_c \qquad ; \qquad (\phi = 0.85) \qquad (3.37)$$

3. Stirrup Spacing (s_v):

Minimum value from

$s_v = \frac{A_v f_y d}{V_s}$

or $s_v = d/2$

or $s_v = 24$"

If V_s exceeds $4\sqrt{f_c'}bd$, stirrup spacing to be provided is $d/4$.

Horizontal Shear :

1. Horizontal Shear Force (V_h): Total horizontal shear to be resisted by stirrups is the smaller value from the two equations :

$$V_h = \frac{A_s f_y}{2} \qquad ; \qquad V_h = \frac{0.85 f_c' A_c}{2} \qquad (3.38)$$

2. Stirrup spacing (s_h): For #3 bars, shear developed is 3.245 kips. [22]. Hence, the number of studs in the region between maximum positive moment and zero moment is given by

$$n = \frac{V_h}{3.245} \qquad (3.39)$$

where

V_h = smaller value of the horizontal force calculated by Eq. (3.38) in kips.

and the stirrup spacing is given by,

$$s_h = \frac{20}{n} \qquad (3.40)$$

where

s_h = required horizontal spacing, in.

(C) Final Stirrup Spacing.

The final stirrup spacing is the smaller of the two values s_v and s_h.

Chapter 4

EXPERIMENTATION

4.1   GENERAL

This chapter discusses the experimental program of the research. Designation and description of the specimens along with a design summary is provided. The procedure for the construction of the beam specimens and instrumentation used is then discussed. This is followed by a description of the test setup and loading procedure for the ultimate failure test of the specimens.

4.2   DESCRIPTION OF TEST SPECIMENS

The test specimens consisted of three beams with plates of different thickness (varying steel reinforcing ratios). Dimensions for the length, width and depth of the beams were selected to facilitate their construction, handling and testing. The width, total depth and effective span of all the beams were 3.0, 6.5 and 46.0 in. respectively.

The steel reinforcing ratios intended for the three beams were $\frac{1}{3}\rho_b$, $\frac{2}{3}\rho_b$ and ρ_b, but the thickness of the nearest corresponding plate governed these values. Plates of thickness 1/8, 1/4 and 3/8 in. were selected, which resulted in ρ values of 0.34 ρ_b, $0.69\rho_b$ and $1.05\rho_b$. The intended 28-day compressive strength of concrete was 4000

psi. The specimens were designated as follows :

Beam I   Plate Thickness $= 1/8''$ $\rho = 0.34\rho_b$

Beam II   Plate Thickness $= 1/4''$ $\rho = 0.69\rho_b$

Beam III   Plate Thickness $= 3/8''$ $\rho = 1.05\rho_b$

The plate for Beam I after ordering had a thickness of 0.1162 in. The average 28-day compressive strength of concrete obtained was 6250 psi. The increase in the strength of concrete resulted in the following final configuration of the test specimens :

Beam I   Plate Thickness $= 0.11617''$ $\rho = 0.29\rho_b$

Beam II   Plate Thickness $= 0.25217''$ $\rho = 0.67\rho_b$

Beam III   Plate Thickness $= 0.375''$ $\rho = 0.91\rho_b$

4.3   BEAM DESIGN

The beams were designed using the procedure described in Chapter 3. The initial design was based on a steel yield strength of 36 ksi and a concrete compressive strength of 4000 psi. Typical reinforcement details for a beam are shown in Fig 4.1. A summary of the design is available in Table I. A typical design example, Beam III is available in Appendix A.

A revised design (Table II) was performed to check the effect of the changes of the specimen configuration on the the initial design. The stirrup spacing was checked, since it was the main design variable. It can be observed from Table I and Table II that the spacing required for horizontal shear considerations changed. However, spacing due to vertical shear controlled the design of all the beams. Since no change in spacing due to vertical shear was obtained for any beam, it was concluded that there would be no appreciable change in the flexural behaviour of the beams.
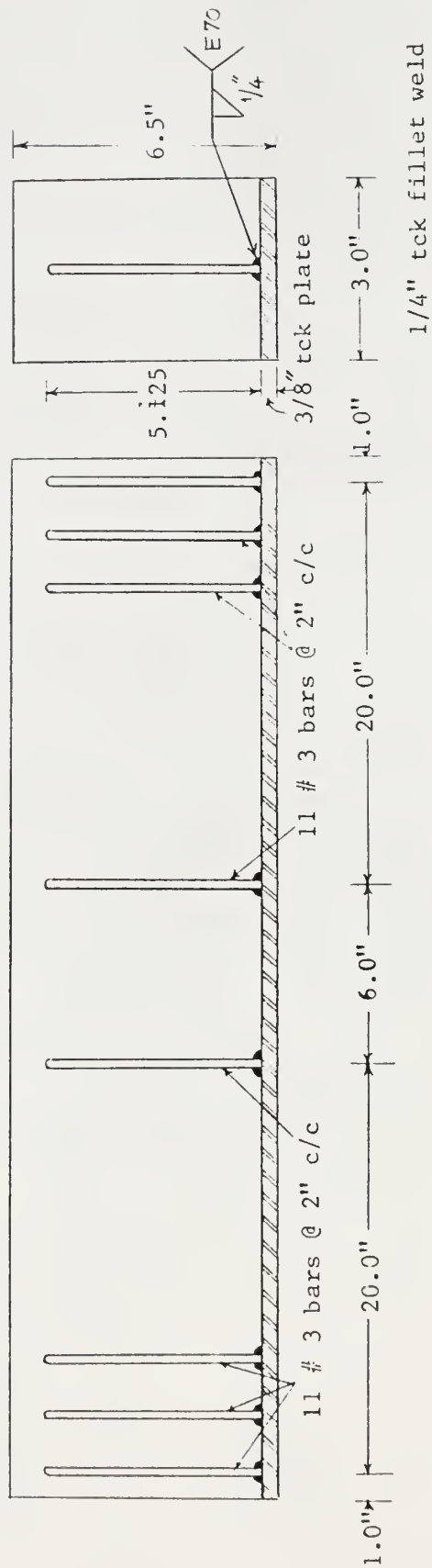
Figure 4.1: Typical Reinforcement Details of a Beam.

TABLE I

DESIGN SUMMARY (OLD)

No.	Item	Unit	Specimen Type		
			Beam I	Beam II	Beam III
1	Plate Thickness	in	0.125	0.250	0.375
2	Steel Reinforcing ratio in terms of ρ_b		0.34	0.69	1.05
3	Design Ultimate Moment Capacity	in_k	70.0	123.0	158.0
4	Design Ultimate Shear Capacity	k	3.5	6.1	7.9
5	Stirrup Spacing (basis of vertical shear)	in	3.0	3.0	1.5
6	Stirrup Spacing (basis of horizontal shear)	in	10.0	4.0	2.5
7	Stirrup Spacing provided	in	2.0	2.0	2.0

$f'_c = 4000\ psi$

$f_y = 36\ psi$

$E_y = 29\ X\ 10_3\ psi$

$E_c = 4.06\ X\ 10_3\ ksi$

$D = 6.5\ in$

$b = 3.0\ in$

$L = 46.0\ in$

$a = 20.0\ in$

44

TABLE II

DESIGN SUMMARY (REVISED)

No.	Item	Unit	Specimen Type		
			Beam I	Beam II	Beam III
1	Plate Thickness	in	0.1162	0.2522	0.3750
2	Yield Strength	ksi	41.3	44.5	40.8
3	Modulus of Elasticity of Steel	ksi	26.5	29.4	29.3
4	Steel Reinforcing ratio in terms of ρ_b		0.29	0.67	0.91
5	Design Ultimate Moment Capacity	in-k	78.0	161.0	201.0
6	Design Ultimate Shear Capacity	k	3.9	8.0	10.0
7	Stirrup Spacing (basis of vertical shear)	in	3.0	1.5	1.5
8	Stirrup Spacing (basis of horizontal shear)	in	6.0	3.0	2.5
9	Stirrup Spacing provided	in	2.0	2.0	2.0

$f'_c = 6250\ psi$

$E_c = 4.06 \times 10_6\ psi$

$D = 6.5\ in$

$b = 3.0\ in$

$L = 46.0\ in$

$a = 20.0\ in$

4.4   BEAM CONSTRUCTION

The beams were constructed in the following stages:

1. Construction of the forms : The forms for all the beams were prepared using 3/4″ thick plywood and were connected by clip angles to a 4′x4′ plywood base board. Fig 4.2 shows a schematic of the formwork assembly and Fig. 4.3, a photograph of the same.

2. Fabrication of the steel cage : The steel cage was prepared by cutting #3 bars to form single legged stirrups of a size that provided concrete cover of one inch. These stirrups were then welded to the base plate according to the design stirrup spacing.

3. Mixing and Placement of the concrete : A concrete mix for an intended 28-day maximum compressive strength of 4000 psi was prepared. It was placed into the forms, and compacted by proper hand tamping especially at the edges and corners of the forms. A light coating of grease was applied to the interior faces of the forms prior to placing of the concrete. Care was taken to not have any grease on the steel plates. The entire setup was then vibrated for 90 seconds and the top surface of each beam was screeded flush. A set of ten 3 x 6 in. cylinders was simultaneously cast along with the beams . Details of the mix design are included in Table III.

4. Curing of the concrete : The beams remained in the forms for a period of 24 hours and were covered with a polyethylene sheet to prevent any drying shrinkage. After a period of 24 hours, the forms were removed very carefully and the three beams along with the concrete cylinders were placed in the curing room for 28 days to gain their full compressive strengths.

49.5″

$\frac{3}{4}$″

4.5″
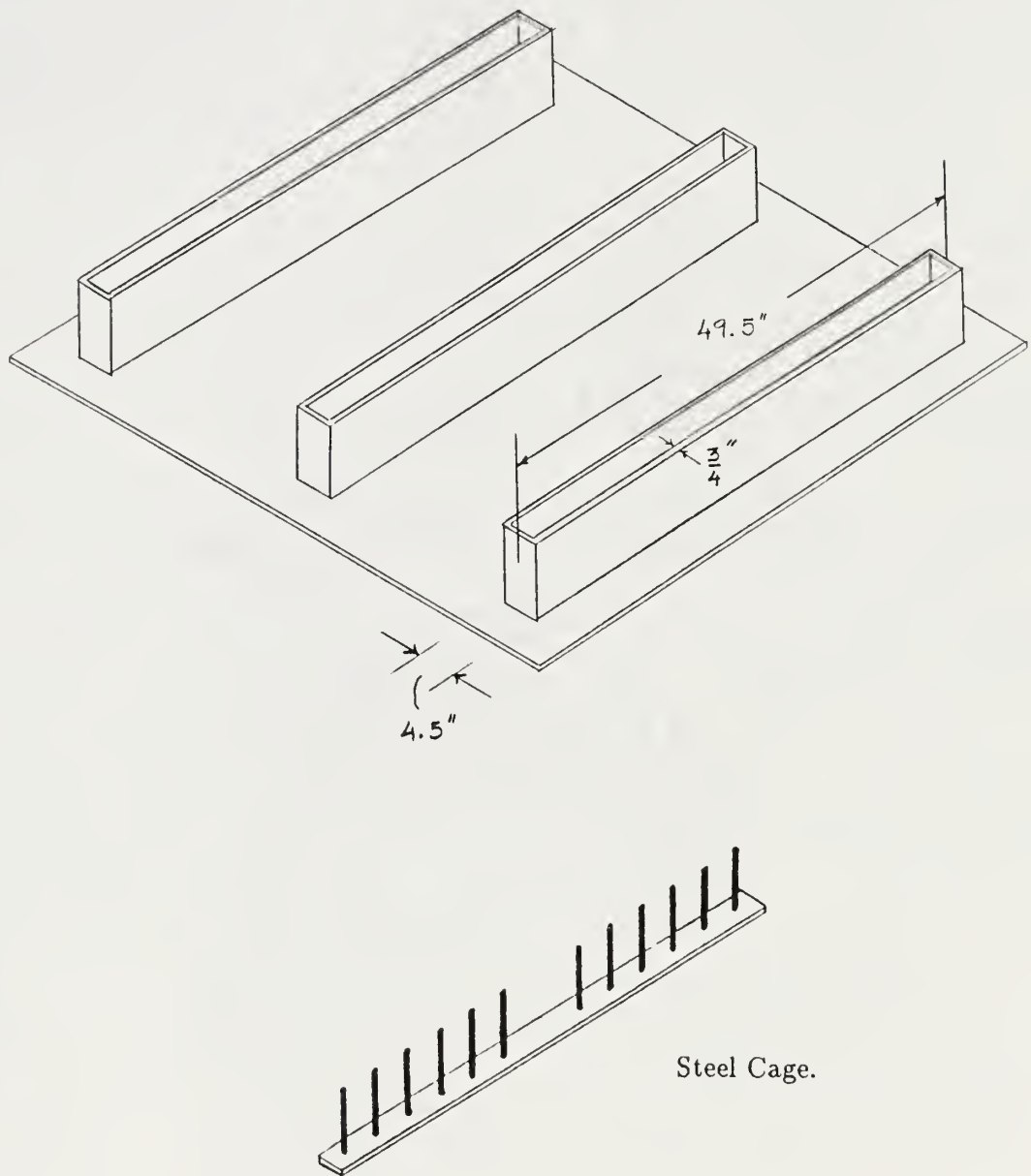
Steel Cage.

Fig. 4.2, Formwork and Steel Cage for the Specimens.
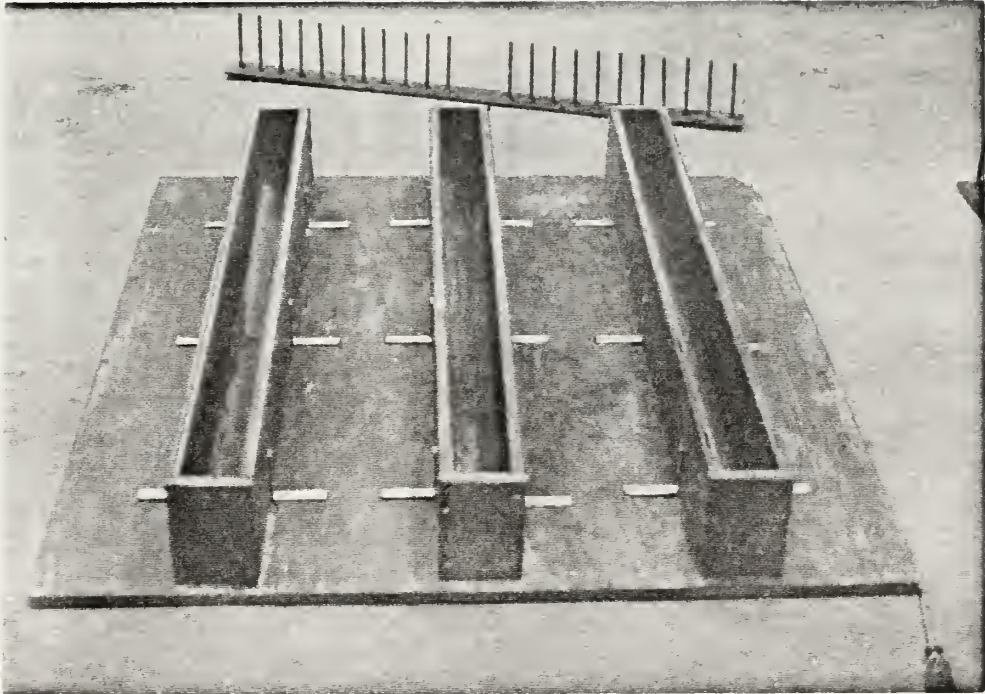
Fig. 4.3, Formwork for all the Beams and Steel Cage for Beam I.

TABLE III

DETAILS OF THE CONCRETE MIX DESIGN

#	Item	Amount for 1 ft^2 (lb)	Amount for 2.4 ft^2 (lb)
1	Water	12.6 lb (5.72)	30.2 lb
2	Cement	22.1 lb (10.2)	53.0 lb
3	Gravel	54.2 lb (24.59)	130.0 lb
4.	Sand	54.1 lb (24.59)	130.0 lb

Values in bracket indicate amounts in kg.

4.5 INSTRUMENTATION

Strains and deflections were measured using strain gages and dial gages respectively. Three student strain gages, manufactured by Measurements Group Inc., North Carolina, 0.12 inches in gage length and of the EA - 06 - 120LZ - 120 series were installed on each beam. Two gages were installed on the top concrete face and one on the bottom steel face.

Gages on the concrete surface were installed using the following procedure: Installing a gage on a concrete surface begins by selecting a small area around the region where the gage is to be installed. This area is ground to a smooth surface with sand paper and/or a grinder depending on the condition of the surface. Liquid epoxy is prepared, and a very small quantity is spread over the ground surface to form a very thin coat of epoxy. After 6 hours, the epoxy will solidify and the coated surface is ground to a smooth finish. The reason for having a smooth surface is to insure a good bond between the material and the gage so that an accurate strain value is obtained. Once the surface is prepared, the gage is installed as per the manufacturer's recommended procedure. The gage on a steel surface is installed similarly except that no epoxy is used. Photographs of the gages on each surface are shown in Fig. 4.4.

Three shielded wires were soldered to the individual strain gages on one end and connected to the Gage Terminal Block of a Vishay/Ellis 21, 10 - Channel Data Acquisition System on the other end. The procedure followed for setting the V/E 21 was as mentioned in the operating manual accompanying the machine. Vertical Deflections were measured at the center of the beam using a dial gage with a least count of 0.001″.
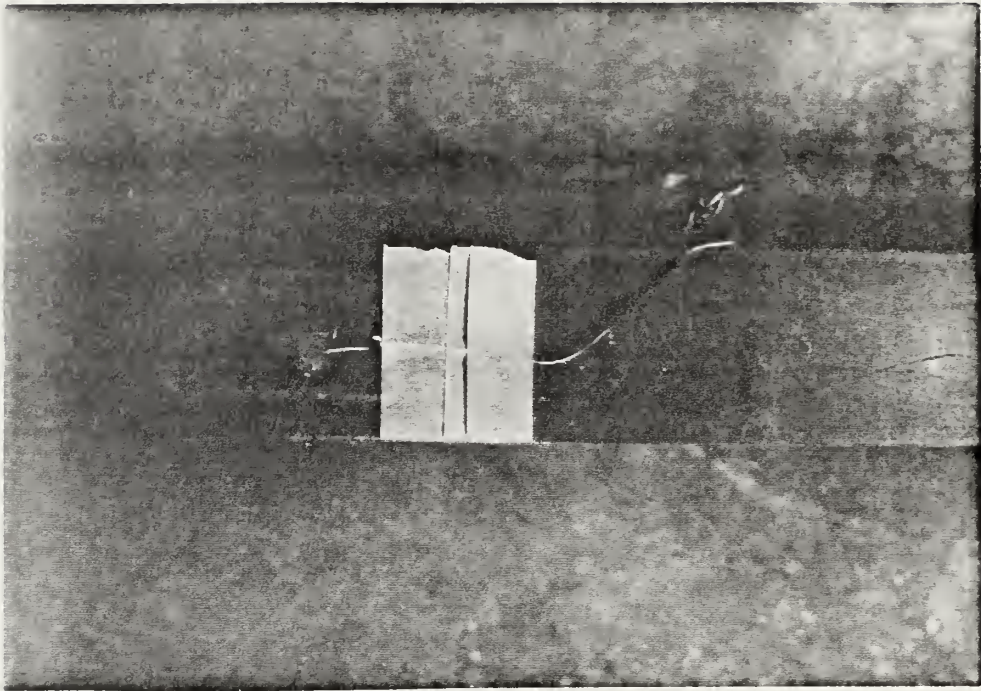
Fig. 4.4, Strain Gage Installed on Concrete and Steel Face of Beam III.

4.6 TEST SETUP

The test was conducted on a Southmark Emery 300,000 lb hydraulic universal testing machine. The test beam was supported on two hinges, which in turn was placed on a W8x18 base beam. A dial gage was placed at the center of the test beam for noting center-line deflections. To create room for the dial gage, steel shim plates were inserted below both the hinges to raise the level of the test beam. A spreader beam was used to provide a four-point bending scheme. The Vishay/Ellis 21 system was stabilized by allowing it to warm up for atleast 15 to 20 minutes prior to loading. During this period, the strain gages were connected to the gage terminal block of the V/E 21 and the machine setting was done. After checking the connections, strain readings and dial gage setting, the beam was ready for loading. A team of four persons were present during testing. A schematic diagram for the entire test setup is shown in Fig 4.5. An overall view of the entire test setup is shown in Fig. 4.6.

4.7 LOADING

The strain gages and dial gages were initialized. A small load was applied to check if appropriate readings were obtained from the gages. Strain readings on the left and the right gages on the top concrete surface of the beam were checked to see if they were equal. If the difference was found to be significant, the beam was adjusted slightly by changing the level of the beam. Prior to the ultimate failure test, two preliminary tests were conducted in the elastic range.

In the elastic range, BEAM I was loaded to a load of 6 kips and BEAM II and BEAM III to a load of 8 kips. Strains were recorded at a load interval of 1 kip. Strains were also recorded at the same interval while unloading the beam to check for accuracy in the readings and to confirm the elastic linear behavior. All gages were initialised, each time the beam was loaded from zero load. Once a
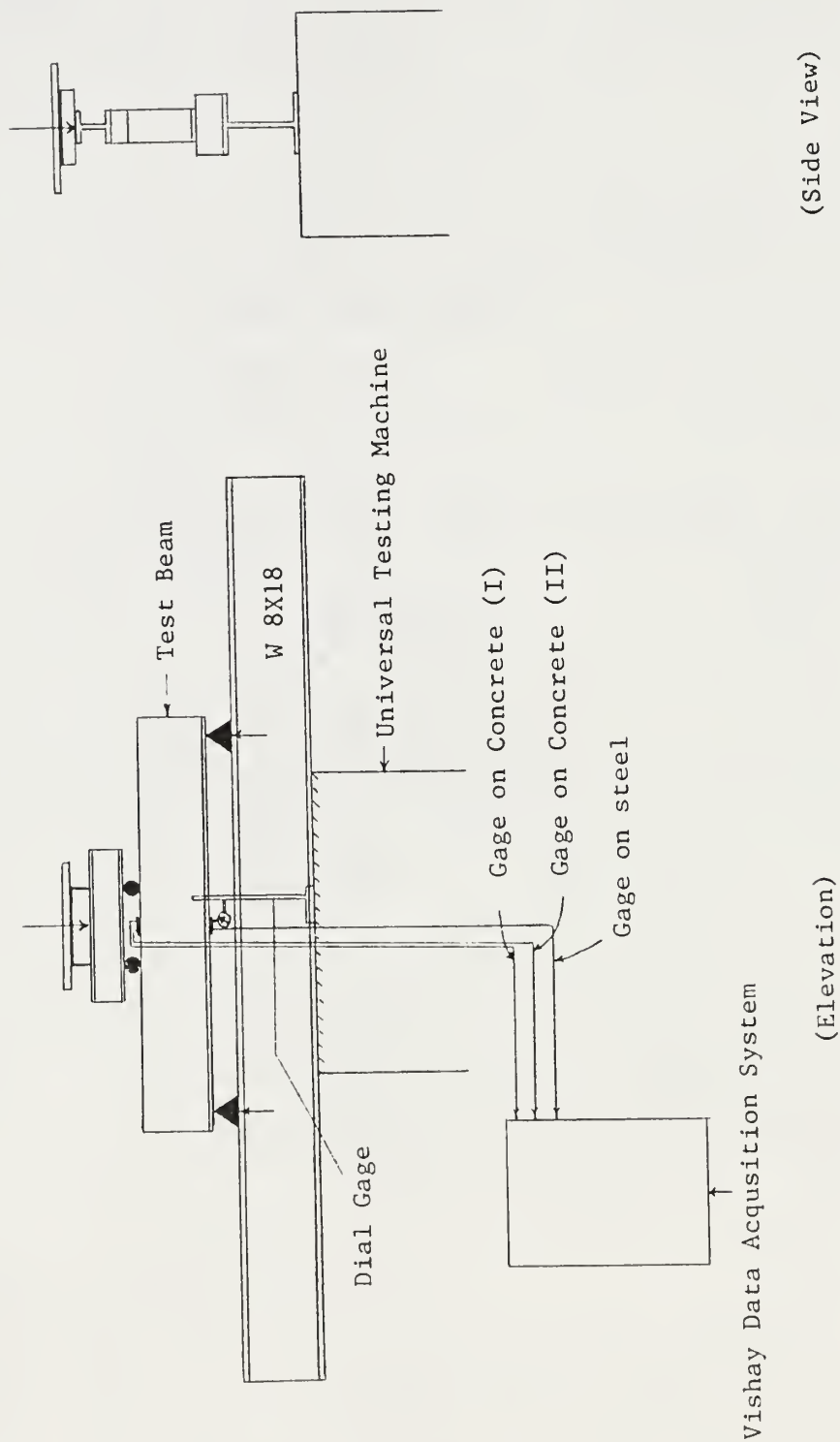
(Side View)
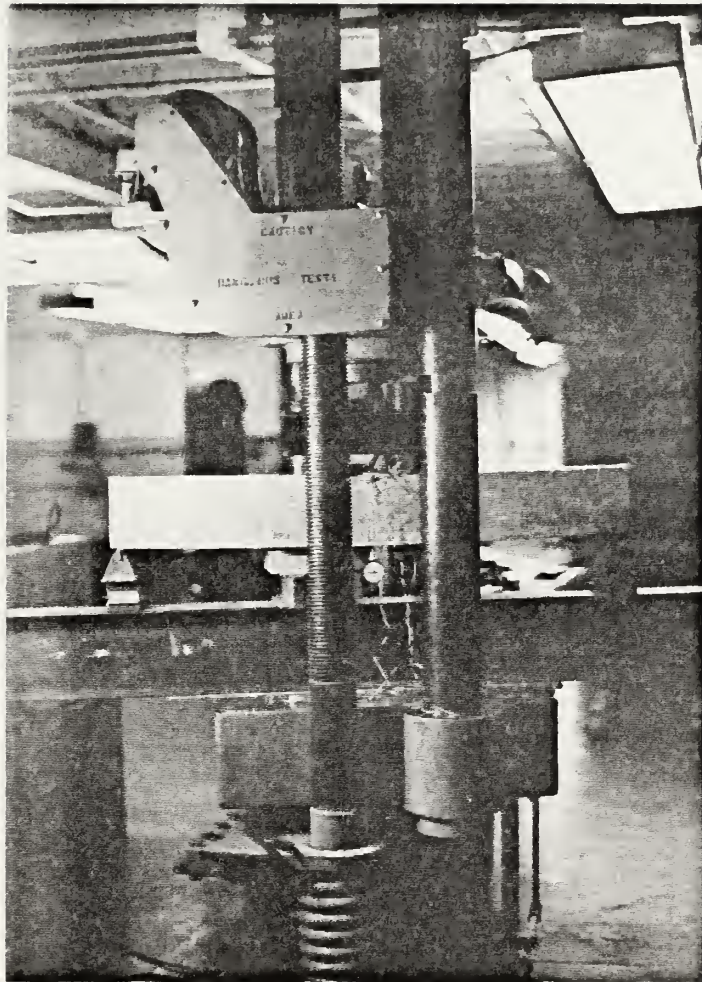
(Elevation)

Figure 4.5: Schematic of the Test Setup.

Fig. 4.6, Overall View of the Test Setup.

linear behavior was observed for the strains in concrete and steel and for the center deflection, the beam was tested for the ultimate failure test.

All gages were once again initialised, and the testing began, but now with load intervals of 2 kips in the elastic range and smaller varying intervals as non-linearity in the material was observed. The reason for the small load intervals was that at higher loads, small increments in the load would cause a large increase in the corresponding strain or deflection. Cracks began to develop in the concrete as the loads were increased and significant ones were marked as they progressed, along with their corresponding load values. The failure mode in all the three beams was a function of the amount of steel reinforcement present in the beam. In BEAM I $(0.29\rho_b)$ and in BEAM II $(0.67\rho_b)$, the steel was first to yield, accompanied by a sudden increase in deflection and followed by crushing of the concrete. In BEAM III $(0.91\rho_b)$, steel yielded almost simultaneously along with crushing of the concrete . The ultimate failure of the beams which occured due to the crushing of the concrete was not disastrous as anticipated, probably due to the presence of the steel plates. In the event of a disastrous failure, adequate arrangement in the form of standby supports was provided to protect the dial gage from damage. Photographs of the failed specimen were taken after the test.

4.8   MATERIALS TESTING

Nine 3 x 6 in. concrete cylinders were tested for their maximum compressive strengths. Stress-strain behaviour was noted for 5 cylinders. Details of the results obtained are discussed in the next chapter.

Three standard steel coupons (ASTM-A 370), with a gage length of 2.0″ were cut out from each steel plate. They were tested for their tensile properties based on the above mentioned ASTM specifications.

Chapter 5

RESULTS, ANALYSIS, AND COMPARISONS

5.1 GENERAL

This chapter discusses experimental and analytical results. The material properties of steel and concrete are provided. Experimental results are studied in the elastic and ultimate range for load-strain behaviour, load-deflection behaviour, cracking patterns, and the overall flexural behaviour of the beams. Analytical results comprise of various kinds of analyses performed on the beams. Results from analysis are then compared with the experimental results.

5.2 MATERIAL PROPERTIES

Results from the compression tests of nine 3 x 6 in. concrete cylinders are presented. The average cylinder strength obtained from the nine tests was 6250 psi. Elongations measured by dial gages for five cylinders are shown in Table IV. Inconsistent data from the tests of three cylinders were rejected. A second-order curve fit was applied to the average values of elongations from the remaining two cylinder tests . Strain gages yield more accurate values, as compared to dial gages, and are recommended for future tests. The resulting stress-strain curve along with its equation and corelation coefficient is shown in Fig 5.1. The modulus of elasticity of the actual

TABLE IV

LOAD ELONGATION VALUES FROM CYLINDER TESTS

Load (kips)	Elongation ($X\,10^{-3}$ inches)					Avg. with Initial Correction
	Cyln-1	Cyln-2	Cyln-3	Cyln-4	Cyln-5	
0	0	0	0	0	0	0
5	0	0	1	0	0	11
10	7	3	2	1	1	21
15	21	17	11	6	4	31
20	33	31	13	18	16	41
25	52	50	20	28	26	51
30	66	69	35	42	41	68
35	78	94	52	62	62	86
40	94	122	78	92	88	108
41.0				120		
41.5					126	
45.0	132	164	104			148

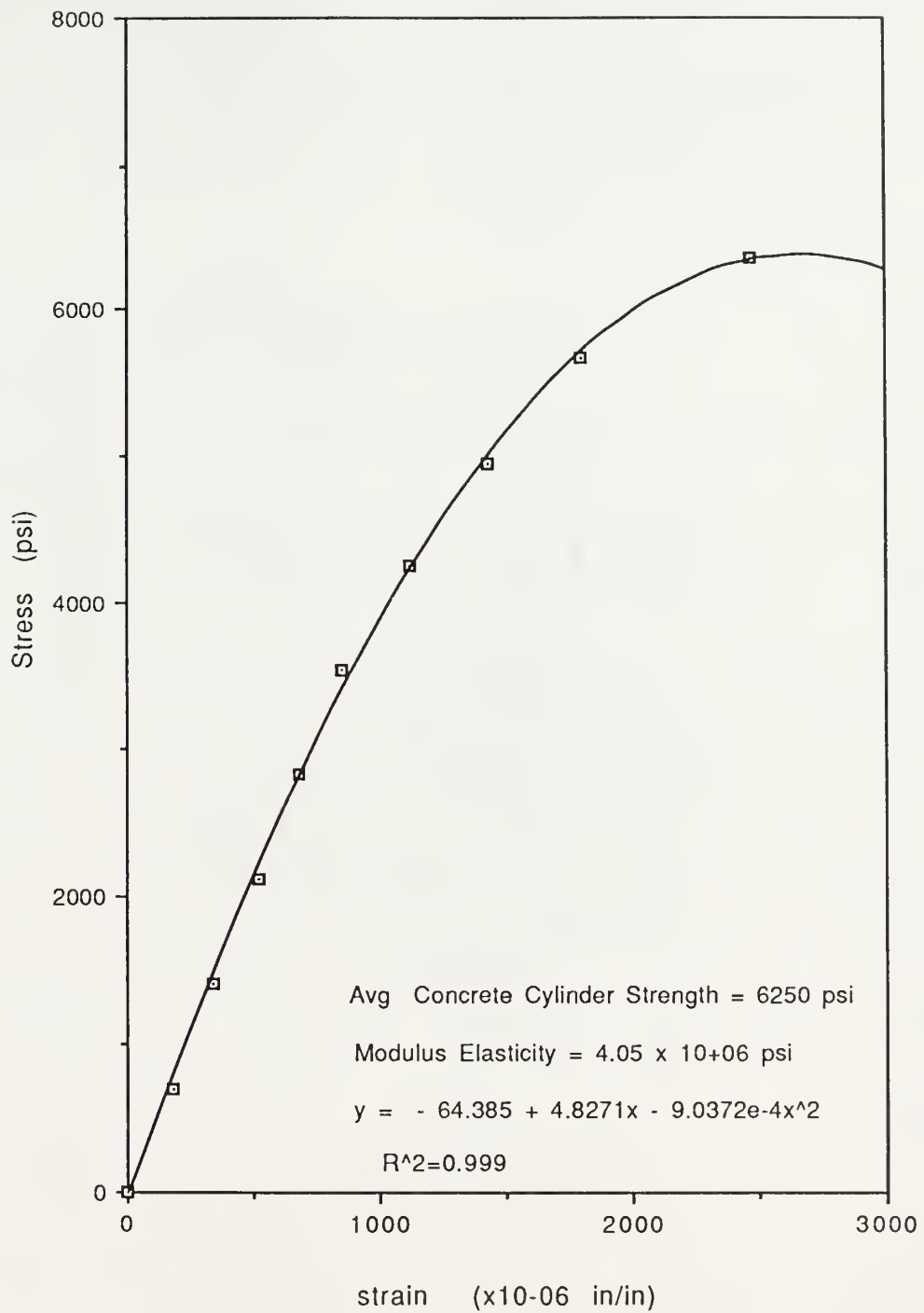Data from cylinder III, IV and V were rejected.

Fig 5.1, Stress Strain Curve for Concrete

58

curve was compared with the (ACI-8.5.1) recommended equation, the Hognestad equation and Carasquillo equation [27]. Details are provided in Table V. It shows that the ACI equation is over conservative for the value of E_c and that Carasquillo's equation gives a good estimate.

Results of the steel coupon tests with final tensile properties are provided in Table VI. A typical stress-strain curve for a steel coupon is shown in Fig. 5.2.

5.3 ELASTIC RANGE STUDIES

5.3.1 Experimental Results

Load-strain and load-deflection variations from the tests of each beam are plotted in Fig 5.3 and 5.4 respectively. Certain observations can be made from the plots.

For the first elastic test, the total load at which tensile cracking of the concrete occured can be observed to be at 2000 lb for Beam I, 3000 lb for Beam II and between 4000 to 5000 lb for Beam III. The load-strain and the load-deflection curves show an abrupt change in slope at the cracking load. Theoretically, the stiffness of a beam must reduce after cracking. However, it is observed that even after cracking occured, all of the stress-strain curves maintained the same slope as exhibited by the concrete when uncracked.

For the second elastic test, a part of the concrete in the tension zone was already cracked. The load-strain and the load-deflection curves, clearly follow a straight line path. Since, the cracking of concrete in the tension zone had already taken place during the first elastic test, no change in the slope is observed.

TABLE V

RESULTS OF COMPRESSIVE STRENGTH FROM CYLINDER TESTS

Cylinder #	Ultimate Loads (kips)	Maximum Compressive Stress (psi)
1	45,000	6365
2	45,000	6365
3	45,000	6365
4	41,000	5800
5	41,500	5870
6	45,800	6478
7	44,000	6223
8	45,000	6365
9	45,000	6365

Average $f'_c = 6250$ psi

Modulus of Elasticity of the Concrete

E_c (ACI) $= w_c^{1.5} \, 35 \, \sqrt{f'_c} = 143^{1.5} \, 35 \, \sqrt{6250} = 4.46 \, X \, 10^6$ psi

E_c (Actual Test) $= 4.05 \, X \, 10^6$ psi

E_c (Hognested) $= 4.67 \, X \, 10^6$ psi

E_c (Carrasquillo) [27] $= 40000 \, x\sqrt{6250} \, x \, 142/145 + 1.0 \, x \, 10^6 = 4.08 \, X \, 10^6$ psi

TABLE VI

RESULTS FROM STEEL COUPON TESTS (ASTM A-370)

Number	Items	Beam-I	Beam-II	Beam-III
1	Throat thickness (in)	0.485	0.496	0.5023
2	Plate thickness (in)	0.1162	0.2522	0.375
3	Area of Section (in^2)	0.485	0.496	0.5023
4	Dynamic yield load (kips)	2.55	5.97	8.43
5	Static yield load (kips)	2.324	5.564	7.69
6	Ultimate load (kips)	3.06	8.1	13.69
7	Strain at yield (in/in)	0.00156	0.00153	0.0014
8	Static yield stress (ksi)	41.27	44.48	40.82
9	Modulus of Elasticity (ksi)	26510	29360	29250

Note : All above values are averages of three coupons tested from each plate
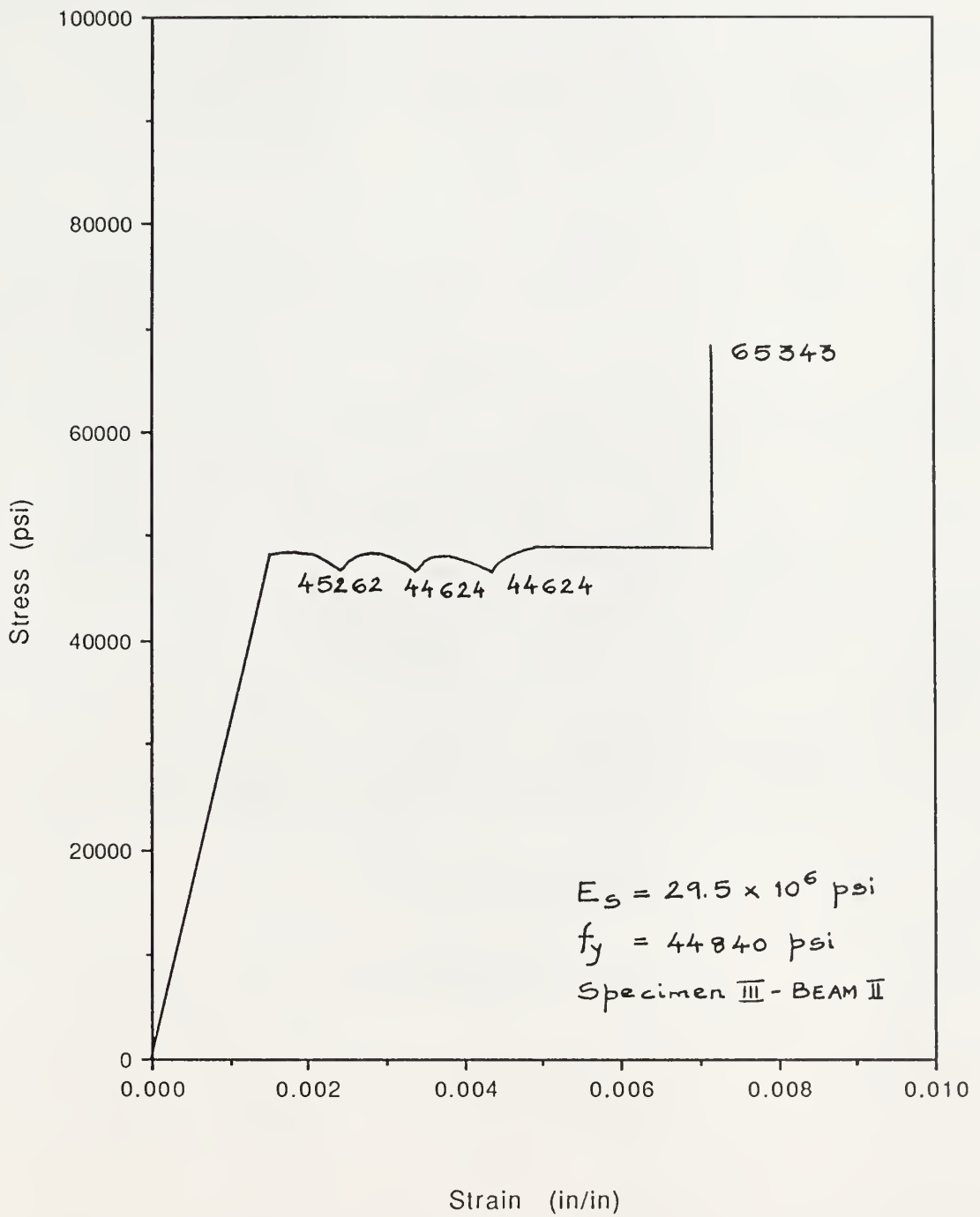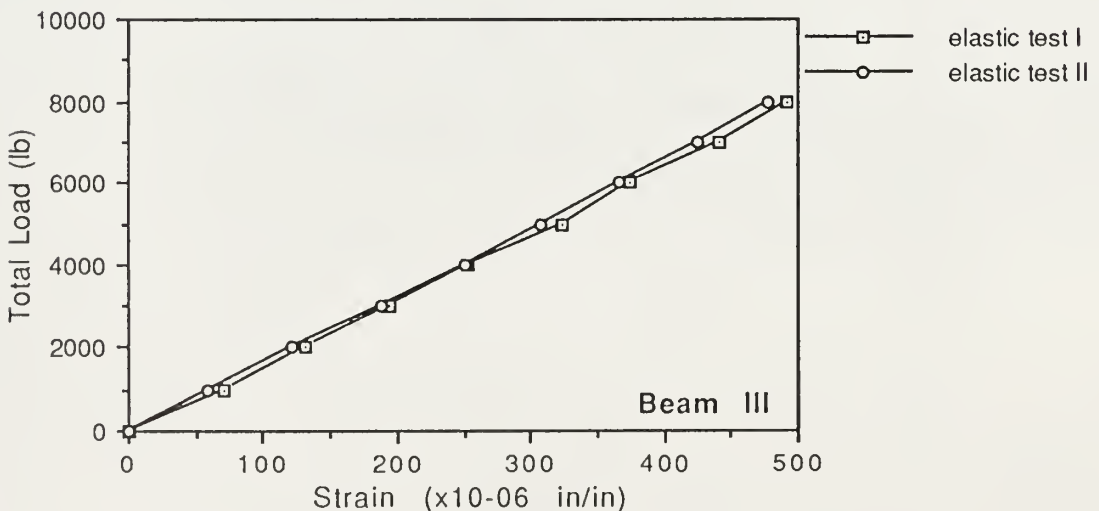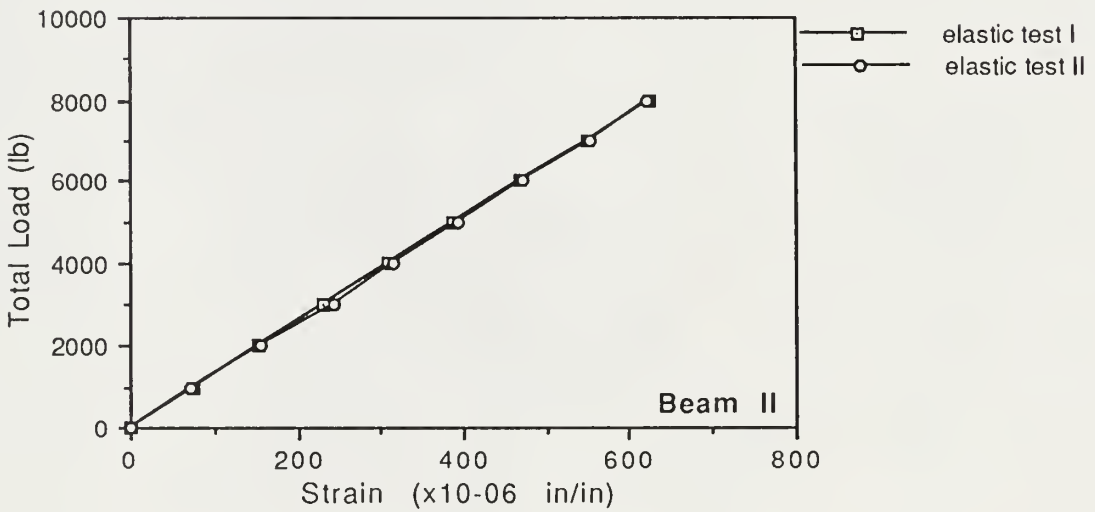
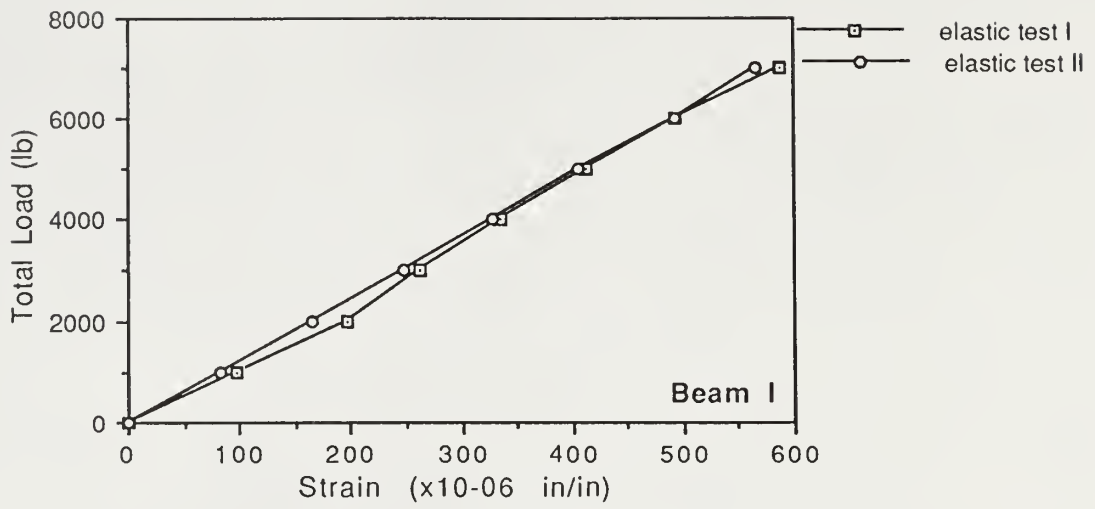Fig 5.2, Typical Stress-Strain Curve for Steel Coupon
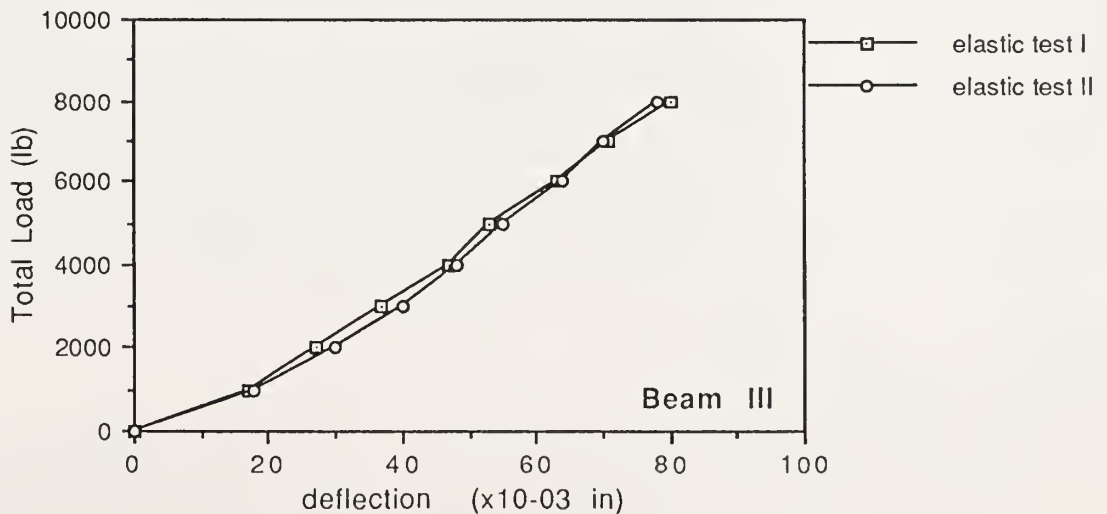
62

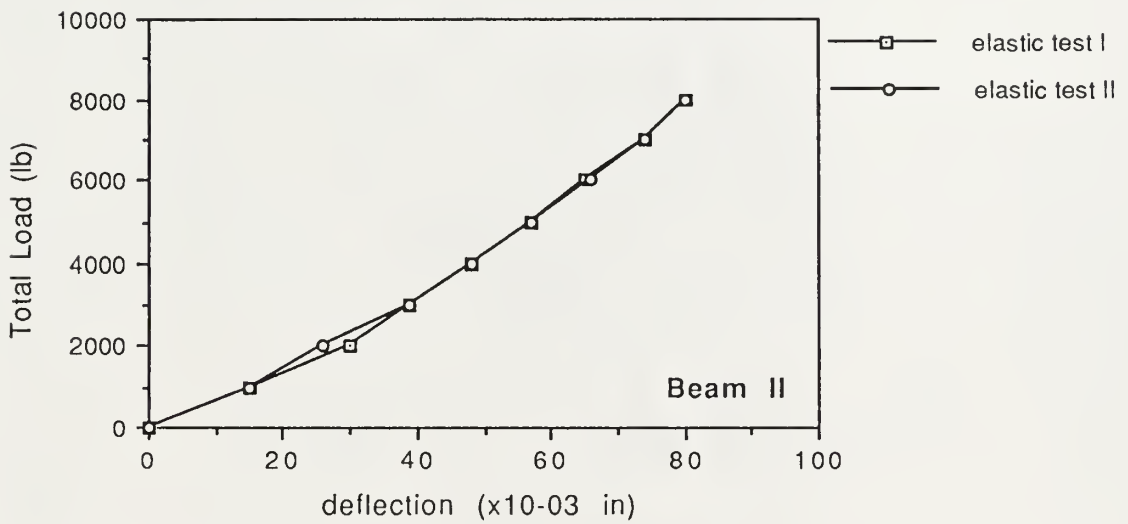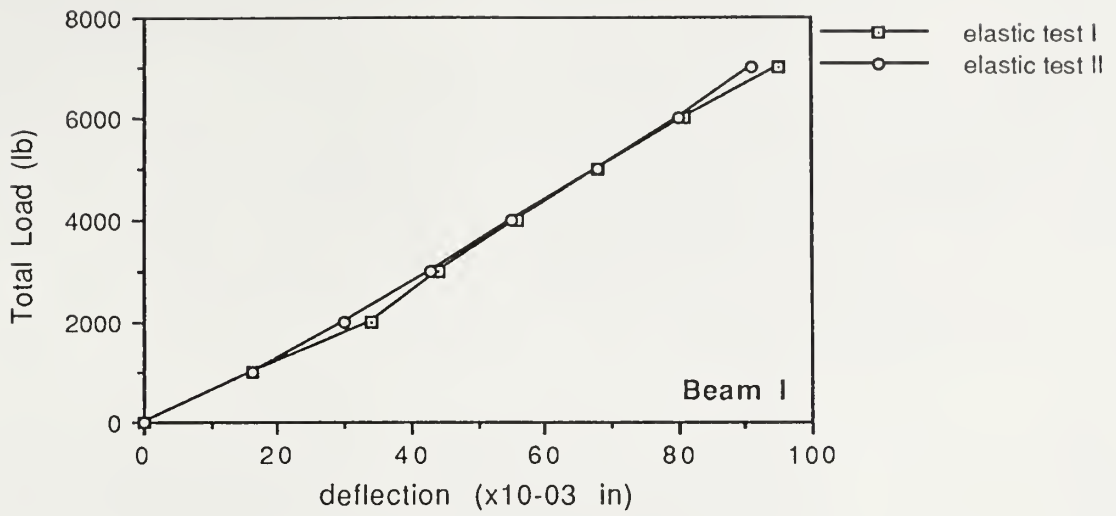Fig 5.3, Load-Strain Behaviour in the elastic range

Fig 5.4, Load-Deflection Behaviour in the elastic range

5.3.2   Elastic Analysis of Elastic Cracked and Uncracked Sections

5.3.2.1   Formulation

An elastic analysis was performed by using a "transformed section" approach. Either a steel or concrete transformed section can be used to yield the same results. The general practice is to use a concrete transformed section for reinforced concrete beams and a steel transformed section for composite beams. In our case, since the beams resembled closely to a composite beam, a steel transformed section was used. The analysis was done for two cases - A) section uncracked and B) section cracked. The steps involved in the analysis were essentially the same in both the cases, except for the Moment of Inertia, which was different. The steps in the analysis, along with the relevant formulae are outlined below for each case :

Case A : Section Uncracked

1. Calculation of Modular Ratio :

   $m = E_s/E_c$

2. Transforming Areas to Steel :

   The transformed area of the section is shown in Fig 5.5. Notations used in the formulae are as shown in the figure.

3. Location of the Neutral Axis :
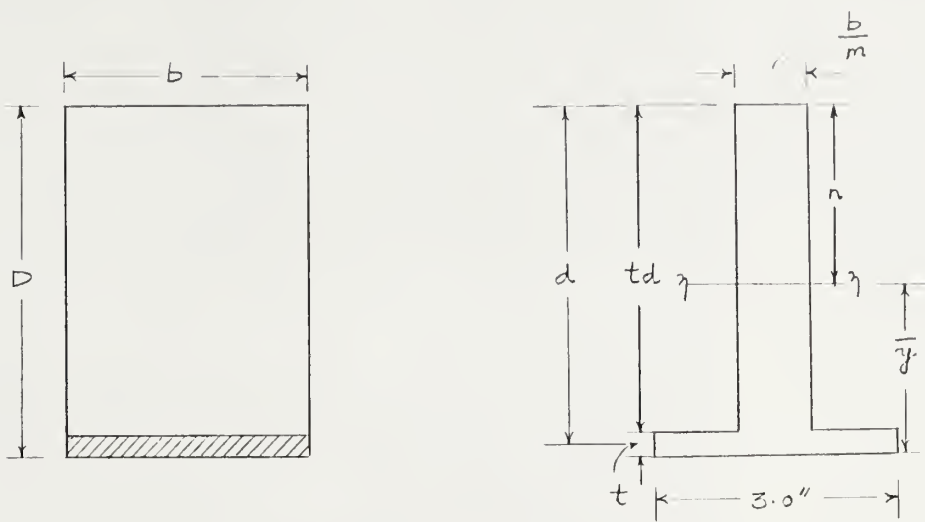
   $A_1 = b.td$
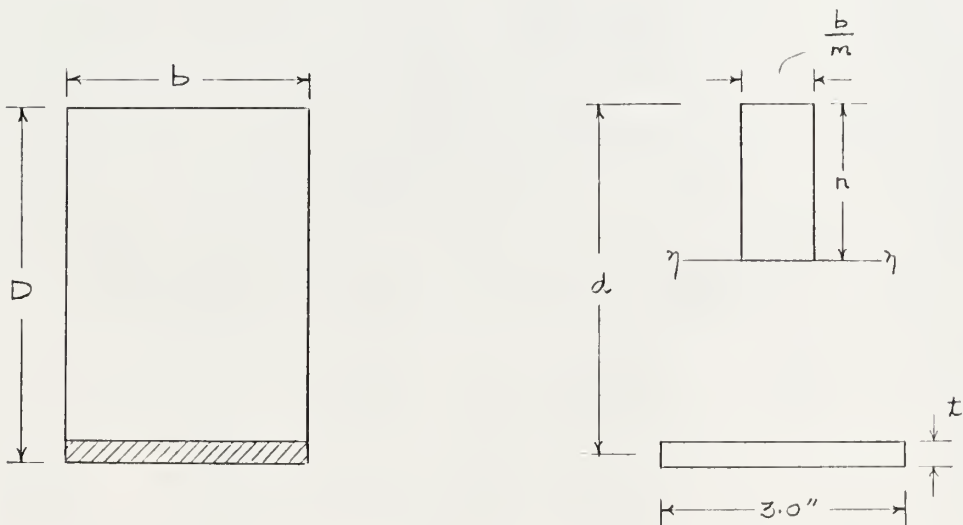
   $y_1 = t + td/2$

   $A_2 = 3.t$

   $y_2 = t/2$

   $y = \frac{A_1 y_1 + A_2 y_2}{A_1 + A_2}$

4. Calculating the Moment of Inertia :

   $I = \frac{btd^3}{12} + A_1(n - td/2)^2 + A_2.(y - t/2)^2$

Case A : Section Uncracked

Case B : Section Cracked

Figure 5.5: Elastic Analysis of Cracked and Uncracked Section.

5. Calculation of the Cracking Moment :

f_r (Modulus of Rupture) $= 7.5\sqrt{f'_c}$ (ACI 9.5.2.3)

$M_{cr} = \frac{f_r.I.m}{y-t}$

6. Calculation of stresses and strains :

Concrete :

$\sigma_c = \sigma_{top} = M_{cr}.n/I.m,$ $\epsilon_c = \sigma_c/E_c$

Steel :

$\sigma_s = \sigma_{bot} = M_{cr}.y/I,$ $\epsilon_s = \sigma_s/E_s$

Case B : Section Cracked

1. Calculation of Modular Ratio :

$m = E_s/E_c$

2. Transforming Areas to Steel :

The transformed section in this case is slightly different. Since the concrete is cracked, the contribution from concrete, below the neutral axis, is neglected. This is not what happens exactly, but it is a reasonable assumption.

3. Location of the Neutral Axis :

Taking the moment of the areas about the neutral axis and solving a quadratic equation for n,

$n = mt[\sqrt{\frac{2d}{mt+1}} - 1]$

4. Calculating the Moment of Inertia :

$I = \frac{n^3}{m} + 3t(d-n)^2$

5. Calculation of stresses and strains :

Concrete :

$\sigma_c = \sigma_{top} = M.n/I.m,$ $\epsilon_c = \sigma_c/E_c$

Steel :

$\sigma_s = \sigma_{bot} = M.(6.5-n)/I,$ $\epsilon_s = \sigma_s/E_s$

In a reinforced concrete beam, the linear elastic range of the beam is generally governed by the behaviour of the concrete rather than that of steel. Most of the time, at a stress in concrete of about $f'_c/2$, the corresponding stress in steel is much lower than its static yield stress. Hence, the maximum elastic moment is calculated as the lesser of the moments corresponding to a stress in concrete of $f'_c/2$ and a stress in steel of f_y, although a check must be made to see which controls.

5.3.2.2 Moment Curvature Plots

To make a comparison between the predicted (analytical) and the experimental results in the elastic range, moment-curvature relations were studied. Fig 5.6 shows moment-curvature plots for each beam. It is observed that all the beams have a greater stiffness compared to the analytical model.

5.3.3 Allowable Stress Analysis

An AISC working stress analysis was performed to check allowable stresses and to determine service load levels. Since the beams were adequately supported while in the curing room, the provisions for shored beams applied. The AISC provisions for composite beams AISC 1.11 [22] permit stresses up to 0.66 f_y for W sections and $0.6 f_y$ for sections such as a steel plate. Corresponding service loads were easily calculated by using the steel transformed section of Case-B (Section Cracked) in section (4.2.2.1). The service loads based on the loading arrangement were calculated as 4.8 kips for Beam I, 10.4 kips for Beam II and 13 kips for Beam III.
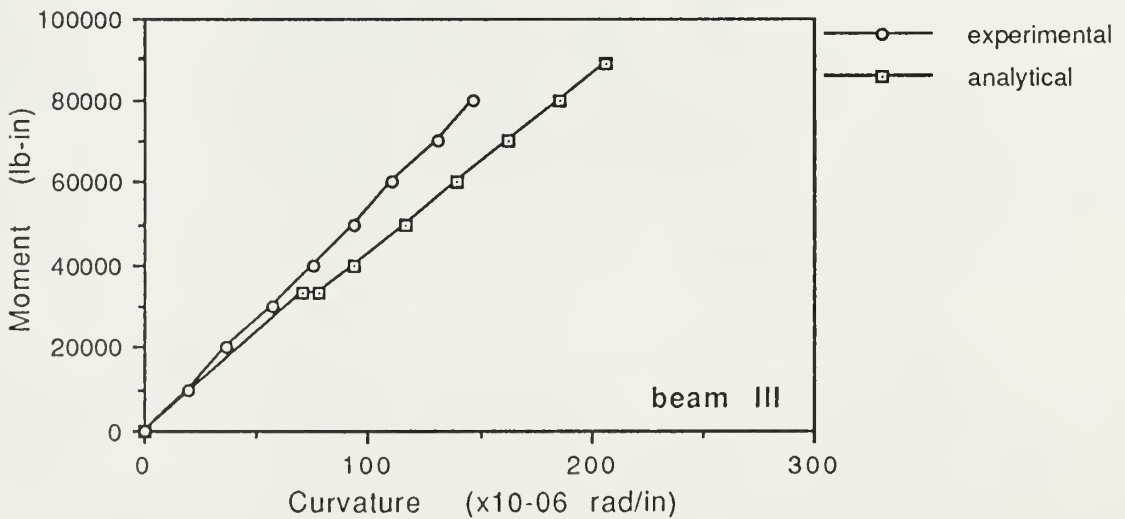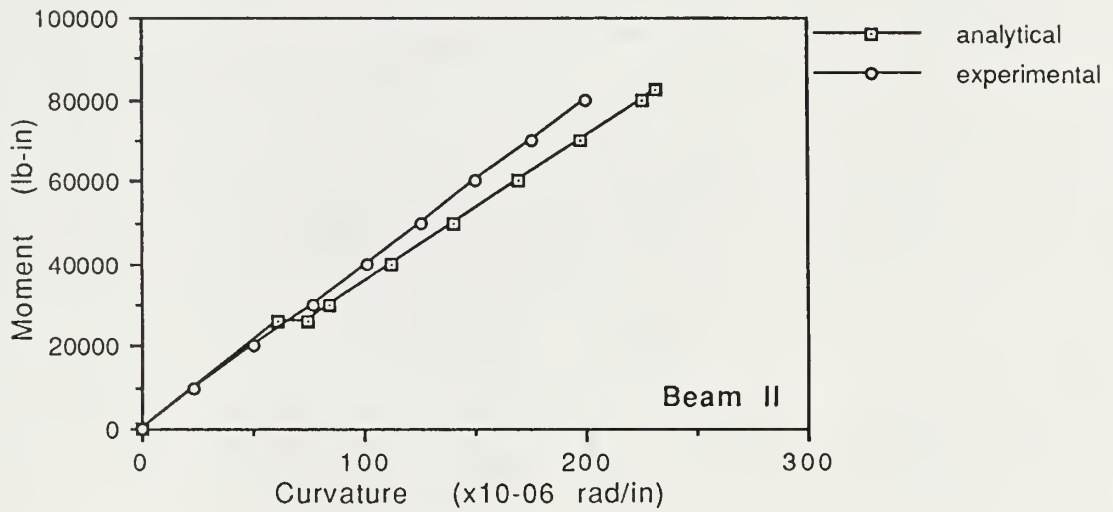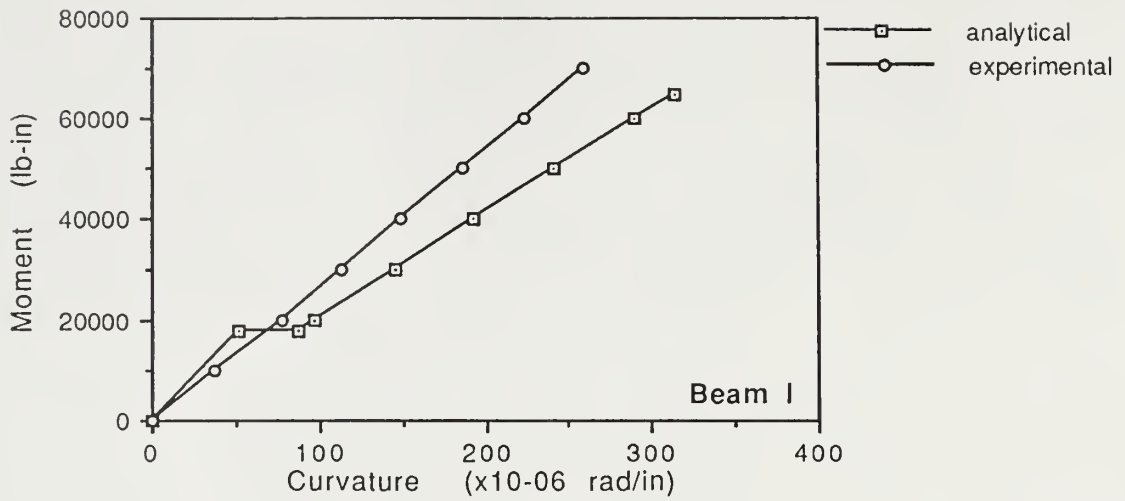
Fig 5.6, Moment Curvature Relationship in Elastic Range

5.4   ULTIMATE RANGE STUDIES

5.4.1   Experimental Results

The ultimate failure load of the beams was governed by the amount of steel rein-
forcement present in the beam.

Beam I with $\rho = 0.29\rho_b$ failed at a total load of 10.8 kips, Beam II with $\rho = 0.67\rho b$
failed at a load of 21.0 kips, and Beam III with $\rho = 0.91\rho_b$ failed at a load of 25.6
kips. The mode of failure in all the three beams was the same, the steel yielded
first followed by the crushing of the concrete - the secondary compression failure.
Load-strain variations in concrete and steel as well as load-deflection behaviour are
described in the following paragraphs.

5.4.1.1   Load Strain Characteristics in Steel and Concrete

Concrete strains measured in the top fiber at the center of each beam are plotted
against the corresponding loads are as shown in Fig. 5.7-5.9. Steel strains measured
at the same location but on the bottom fiber of each beam are also plotted against
the corresponding load in Fig. 5.10.

Concrete strains in Beam I were linear up to a load of 8.0 kips. The first yield of
steel occured at a load of 10.0 kips. Beyond this load the steel became plastic and
the strains in the concrete begin to rise at an increasingly fast rate. The ultimate
failure occured by the crushing of the concrete at a load of 10.85 kips and a concrete
strain of 2910 microstrain.

For Beam II, the concrete was linear up to a load of 12.0 kips. The first yield of
steel occured at a load of 20.0 kips. There was a sudden drop in the steel strain at
this load, possibly due to a redistribution in stresses. The steel became plastic

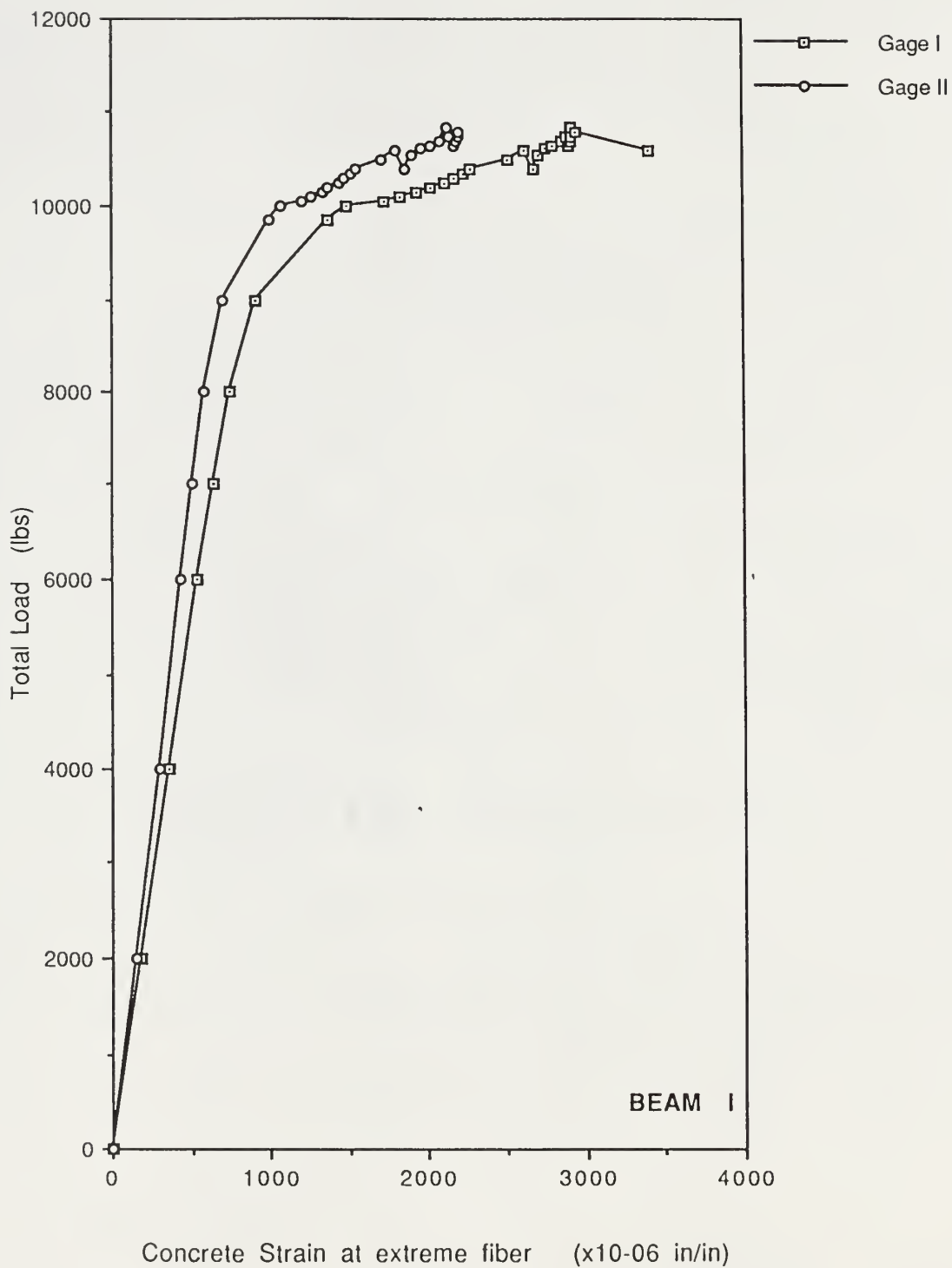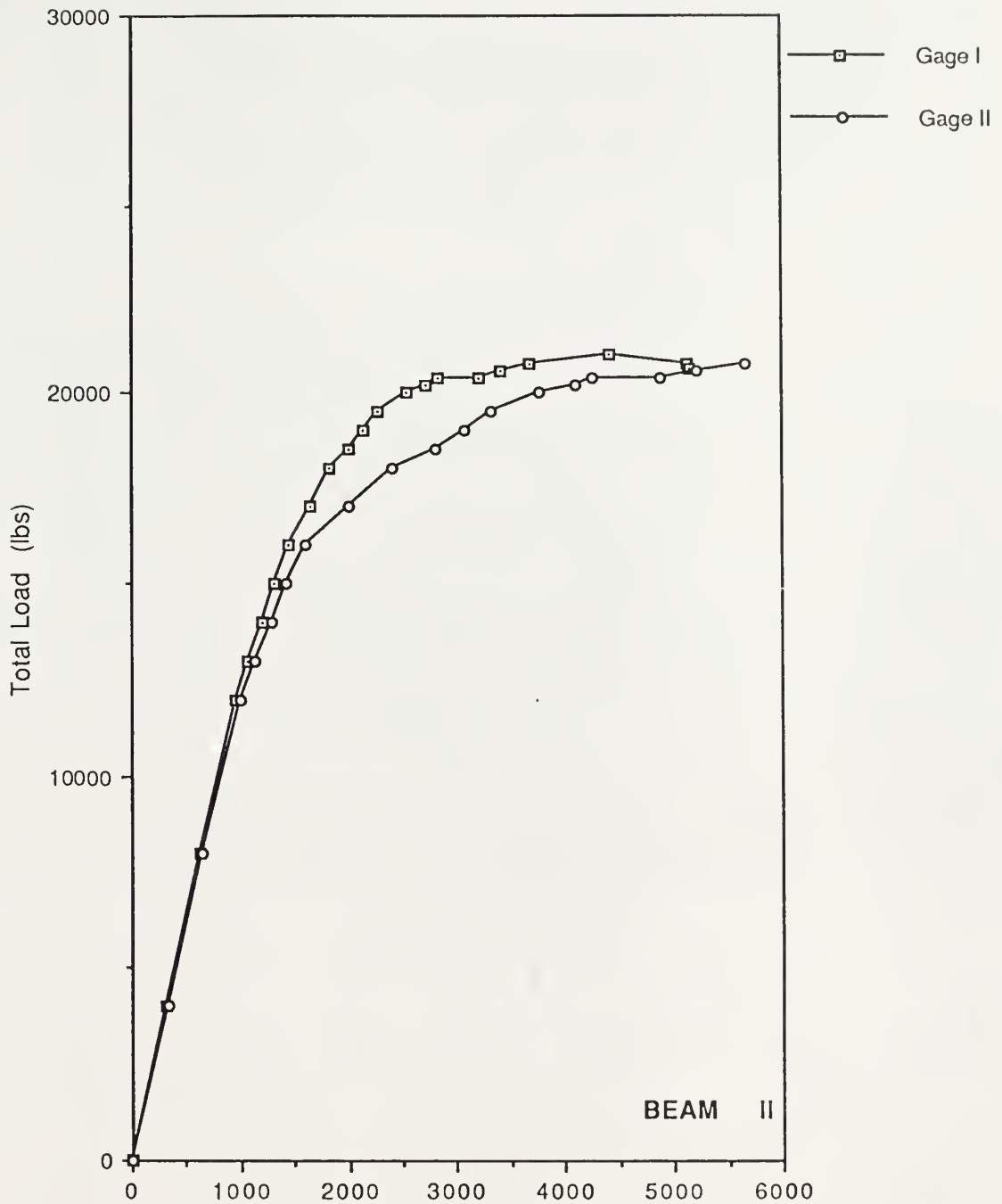Fig 5.7, Load v/s Strain in Concrete for Beam I

71

Concrete strain   at extreme fiber (x10-06 in/in)

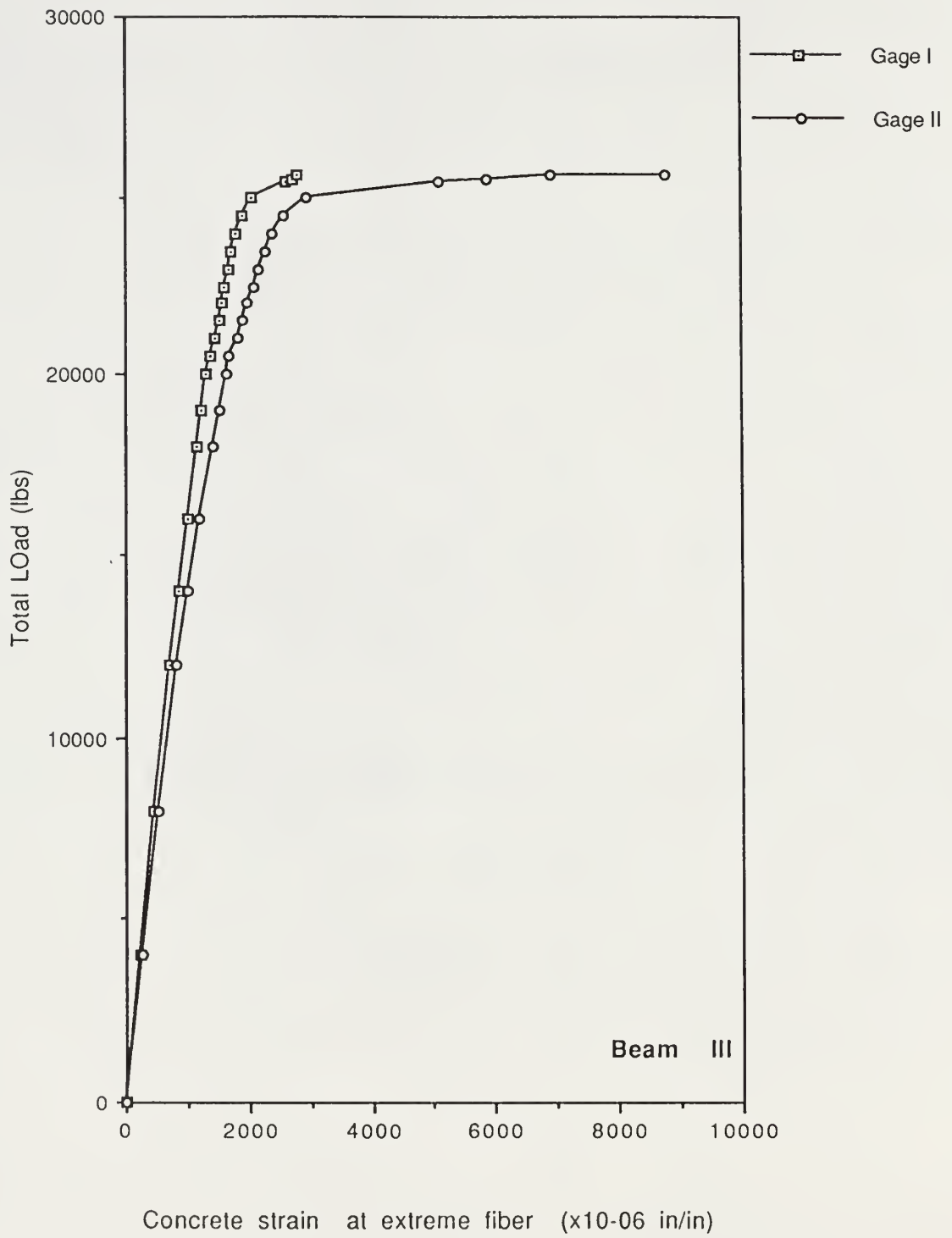Fig 5.8, Load v/s Strain in Concrete for Beam II

72

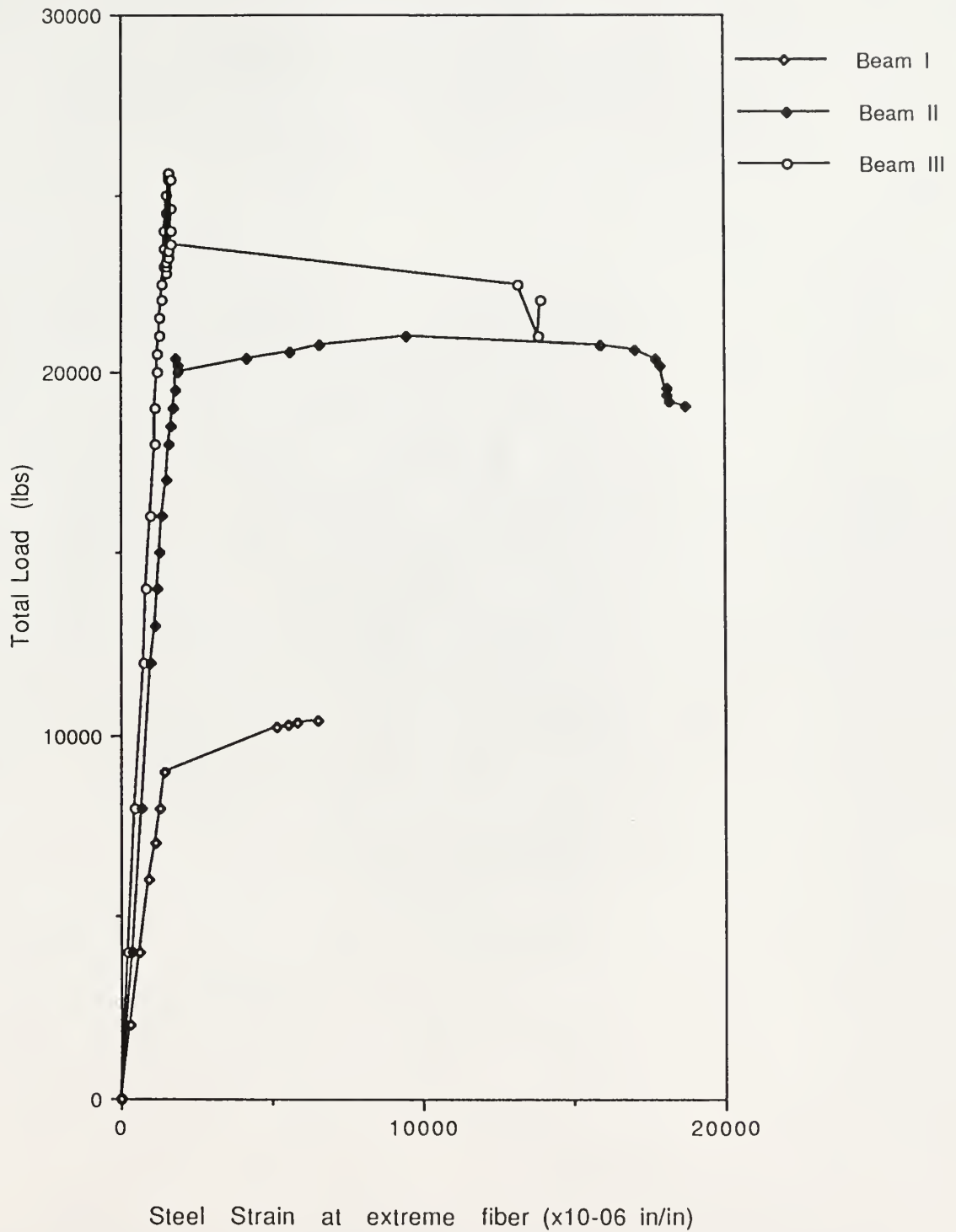Fig 5.9, Load v/s Strain in Concrete for Beam   III

73

Fig 5.10, Load v/s Strain in steel for all three beams

74

at this stage, followed by the concrete which crushed at strains of 4410 microstrain for Gage-1 and 5670 microstrain for Gage-2. The corresponding load at failure was 21.0 kips.

In the case of Beam III, concrete strains were linear up to a much higher load of about 20.0 kips. The steel yielded at a load of 25.4 kips. Since this beam had a high steel reinforcing ratio, almost close to the balanced steel ratio, the failure occured by the simultaneous yielding of the steel in tension and crushing of the concrete in compression. The crushing occured at a load of 25.6 kips. Gage-1 indicated an abrupt failure at a strain of 2800 microstrain, whereas Gage-2 showed a strain of 8790 microstrain indicating a sudden plastic deformation.

5.4.1.2   Load-Deflection Behaviour

The overall behaviour of the beams can be described by the load-deflection variations. The plot for all beams is shown in Fig. 5.11. Ductility of the section can be studied from the load-deflection variation. It can be observed that Beam I showed more ductility, as compared to Beam II and Beam III. Section ductility is the ratio of the curvature at failure to the curvature at first yield. Member ductility is the ratio of the deflection at failure to the deflection at first yield. The member ductilities were,

Beam I - $\frac{0.550}{0.130} = 4.23$

Beam II - $\frac{0.295}{0.143} = 2.06$

Beam III - $\frac{0.315}{0.190} = 1.66$

Another notable feature of the load-deflection variation is the behaviour in the elastic range. All the three beams have almost the same slope in the elastic range. The curves then diverge as ultimate load is reached.
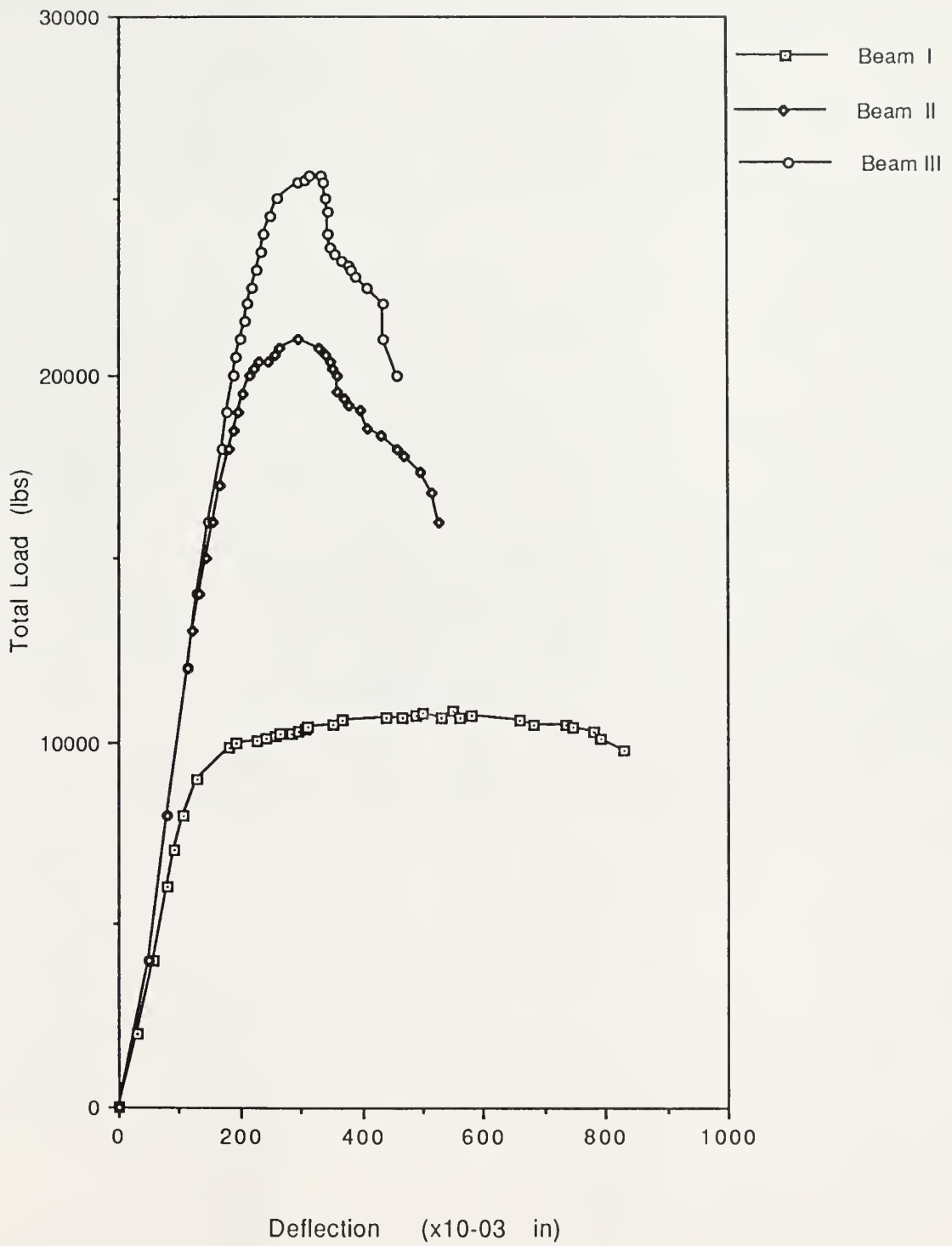
Fig 5.11, Load v/s Center Deflection for all three beams

5.4.2 Analysis of Beams in Ultimate Range

5.4.2.1 General

Two types of analysis were conducted in the Ultimate Range to determine ultimate moment carrying capacities. An ACI-Ultimate Load analysis and a Moment-Curvature Analysis were performed. Details of the analysis are discussed in the following paragraphs.

5.4.2.2 ACI-Ultimate Load Analysis

The ultimate moment carrying capacities and design based on the current ACI Code provisions was discussed in Chapter 3. Since a revised design for the beams was performed earlier, the predicted maximum moment carrying capacity of the beams was known. A comparison between the experimental and ACI-Ultimate moment capacities is provided in Table VII.

5.4.2.3 Moment Curvature Analysis

Moment Curvature Analysis is a rational method for the analysis of reinforced concrete or prestressed concrete beams. It is derived from the basic assumptions about materials and member behaviour. The advantage of the method is that it follows the behaviour of a beam through the entire load range, i.e. from initial loading to failure. Tests have shown the results of this analysis to be reliable. A computer program was written to perform the analysis because of the iterative nature of the method. Following were the assumptions made for the analysis:

1. Changes in strain in the steel and concrete after bonding were assumed to be same.

2. Stress-Strain properties for the materials were assumed to be known.

77

TABLE VII

RESULTS OF EXPERIMENTAL AND ANALYTICAL RESULTS

TYPE		EXPERIMENTAL	ANALYTICAL	%CHANGE
Elastic Analysis (Moment, in-kips)				
	I	80	65	
BEAM	II	120	82	
	III	200	88	
Ultimate Load (Moment, in-kips)				
	I	108	78	39
BEAM	II	210	161	30
	III	256	201	27
Moment Curvature (Moment, in-kips)				
	I	108	87	24
BEAM	II	210	182	15
	III	256	230	11

3. Strains were assumed to be distributed linearly over the depth of the beam.

4. Failure was in flexure. It was assumed that the member did not have a bond or shear failure.

5. The concrete strain at crushing was assumed to be 0.003 in/in and the analysis was terminated at that stage.

The method works on the concept that by knowing the actual properties, i.e. the stress-strain variations of the materials, the moment capacity of the section is determined by actual integration of the stress-strain curve for a desired strain value or curvature at a given section. Hence, for a desired curvature of the beam, the strain in concrete is determined assuming a value for the depth of the neutral axis. Knowing the stress-strain variation in the concrete, the corresponding stress in concrete is known. The total compression in the concrete above the neutral axis is calculated by integrating the stress curve and then comparing it with the total tension force in the steel. If the two values are unequal, the assumed depth of the neutral axis is changed suitably, i.e. if the compression force exceeds the tension force, the depth of the neutral axis is decreased and vice versa. This iteration is continued until both the values become equal. The moment capacity for the given curvature is then obtained by multiplying the compression or the tension force to the lever arm. The above procedure is described in the flowchart shown in Fig. 5.12 for an analysis in the elastic range, i.e. for the preyielding of the steel. Analysis for the postyielding of steel is only slightly different since, the tensile force is now constant. A flowchart for the postyielding analysis is shown in Fig 5.13. A listing of the program for both the cases is available in Appendix B and Appendix C. Results from the analysis are shown in Fig. 5.14-5.16.

Start

---- Mom - Cur - Elastic

Define Variables

Input d_{eff}, E_s, f_y, t

Initialize c=2.0"

ϵ_c = 100, 1700,100

AREA = $\int$ Stress Curve dx
$\overline{y}$ = Centroid of AREA
COMP = AREA * b
ϵ_s = (d-c)/c

$\epsilon_s > \epsilon_y$ — Yes → STOP

No

TEN = ϵ_s*E_s*b*t

(COMP-TEN) < Tolerance

No → COMP>TEN

No → c = c + 0.001

Yes → c = c - 0.001

Yes →

ARM = (d-c) + $\overline{y}$
MOM = (COMP+TEN)*ARM
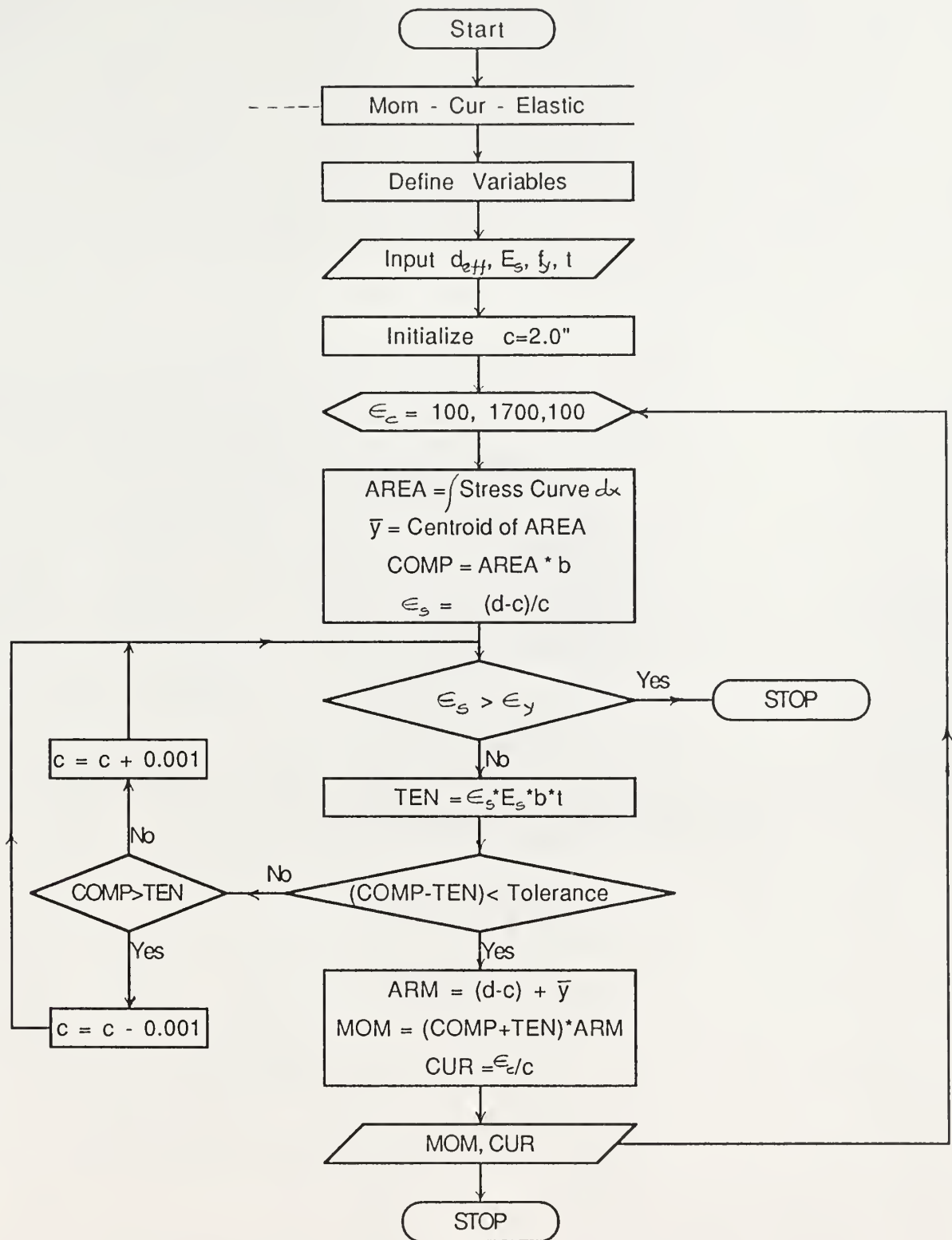CUR = ϵ_c/c

MOM, CUR

STOP

Figure 5.12: Flowchart for Moment Curvature Analysis in the Elastic Range.
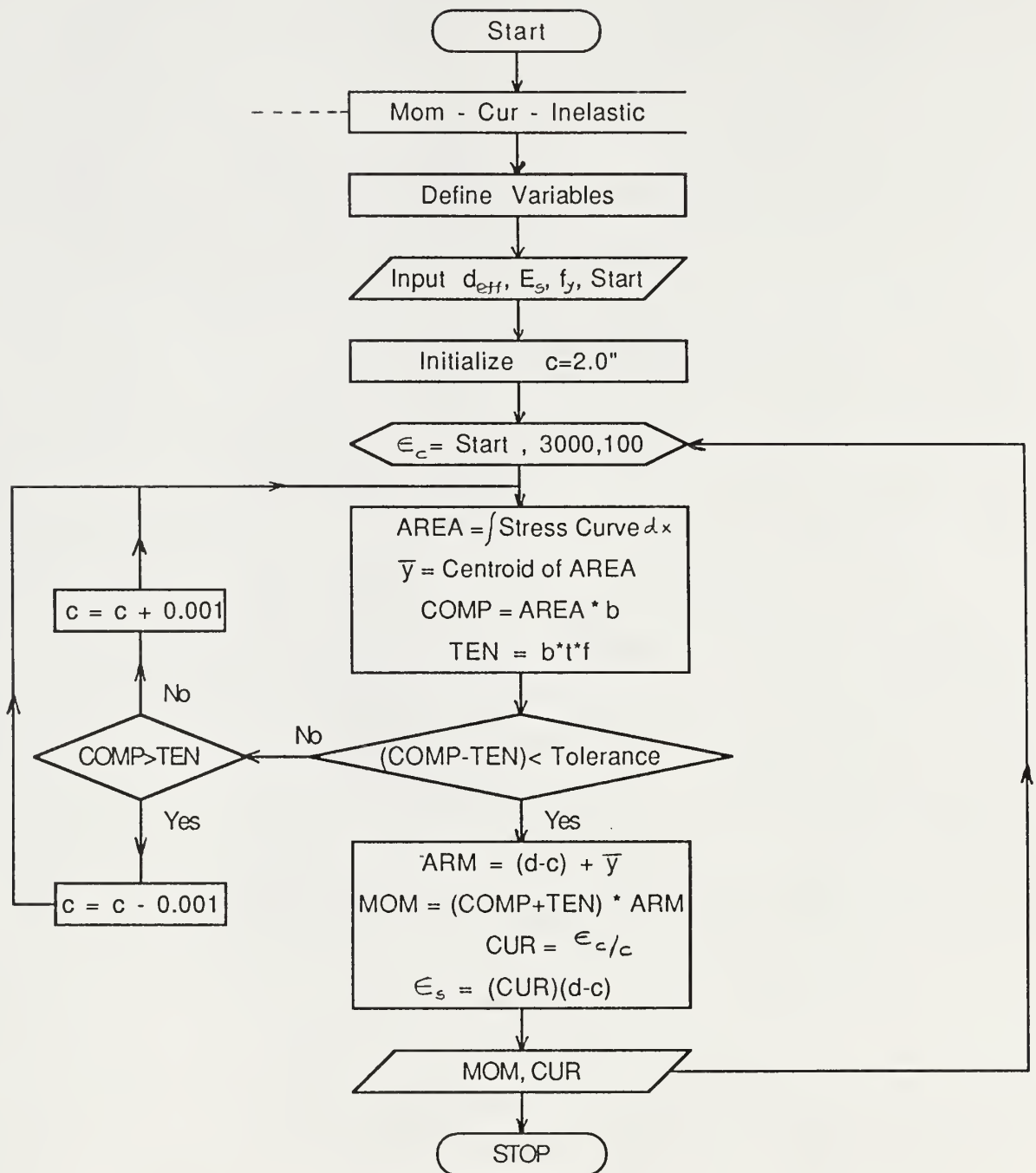
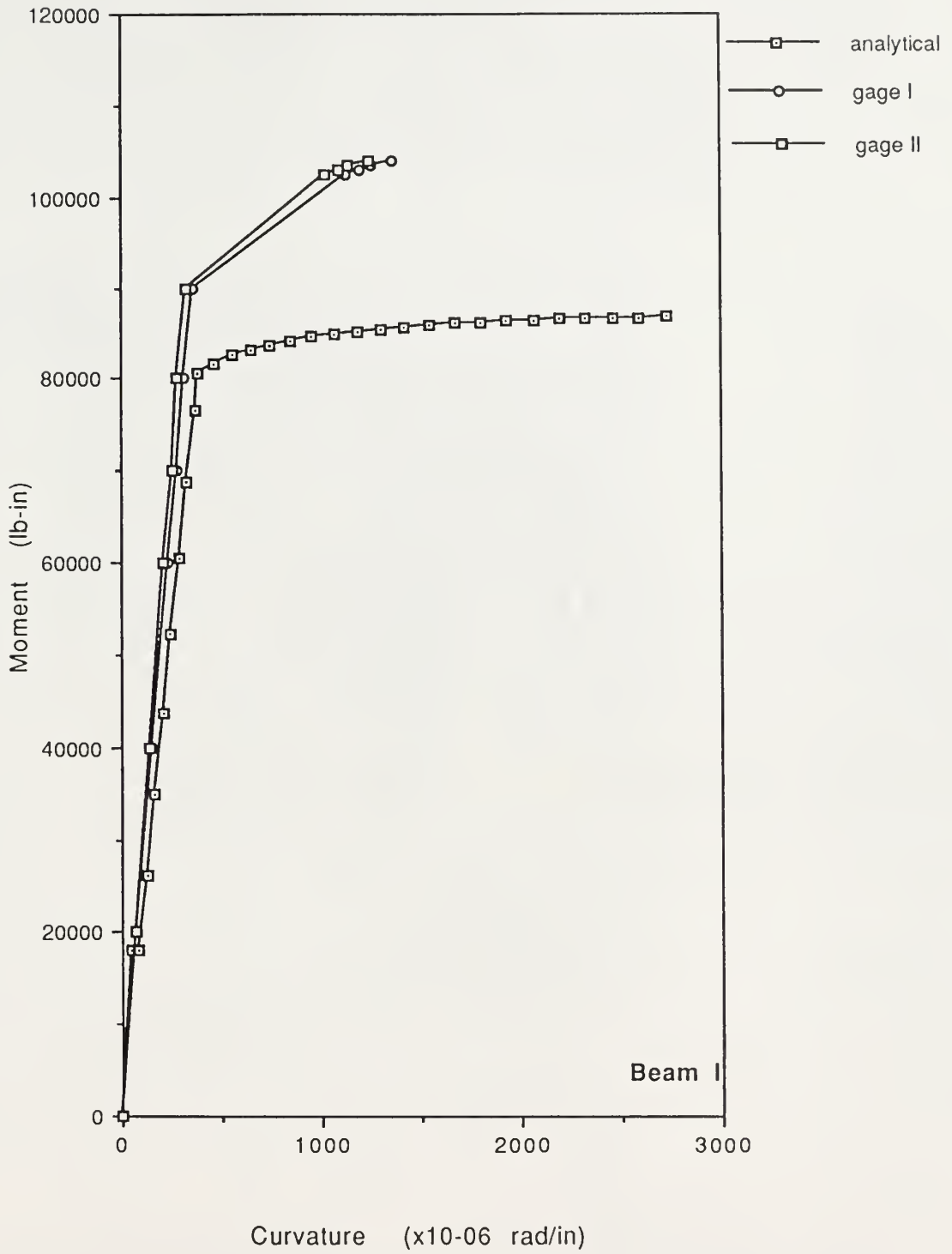Figure 5.13: Flowchart for Moment Curvature Analysis in the Inelastic Range.

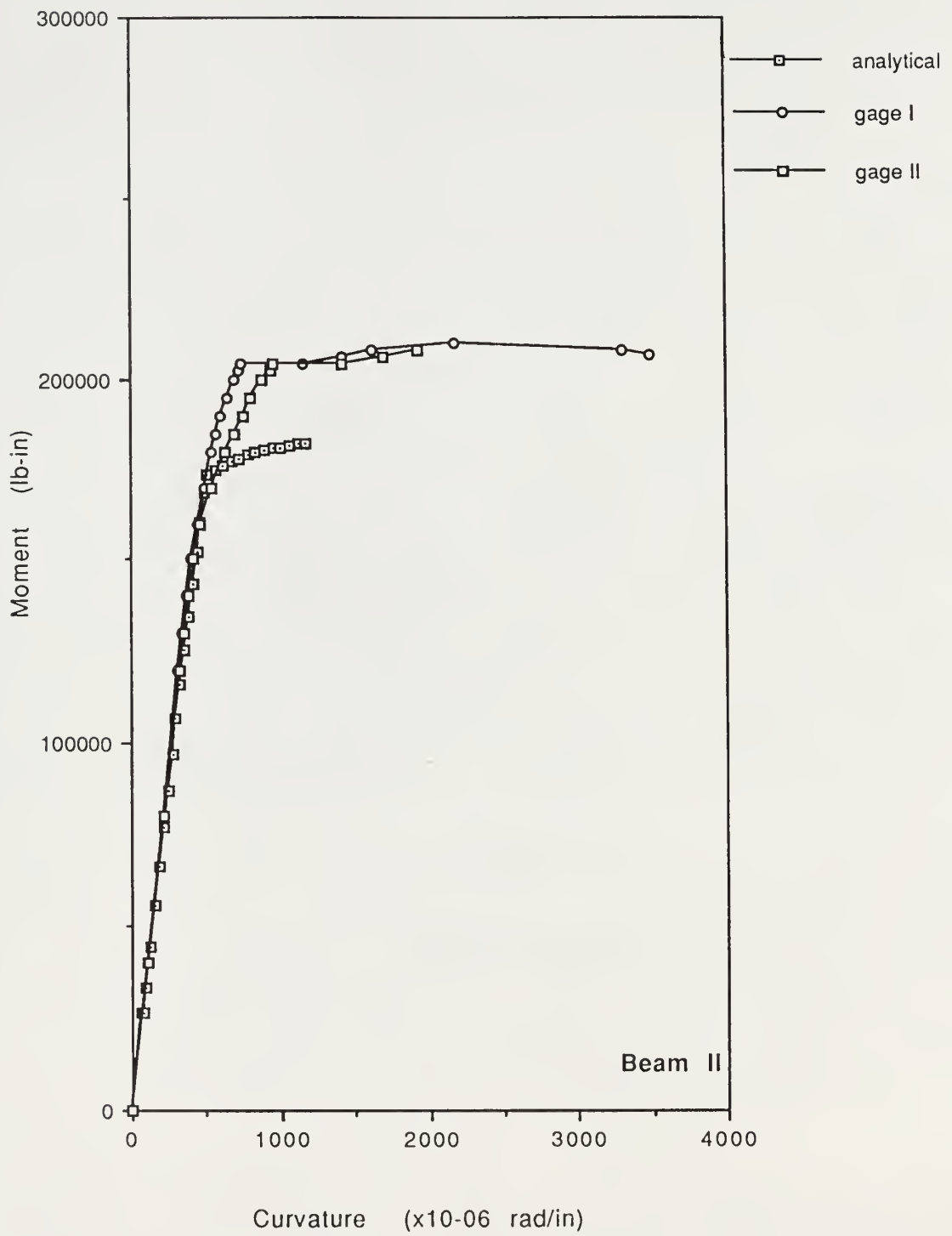Figure 5.14: Moment Curvature Relationship for Beam I.

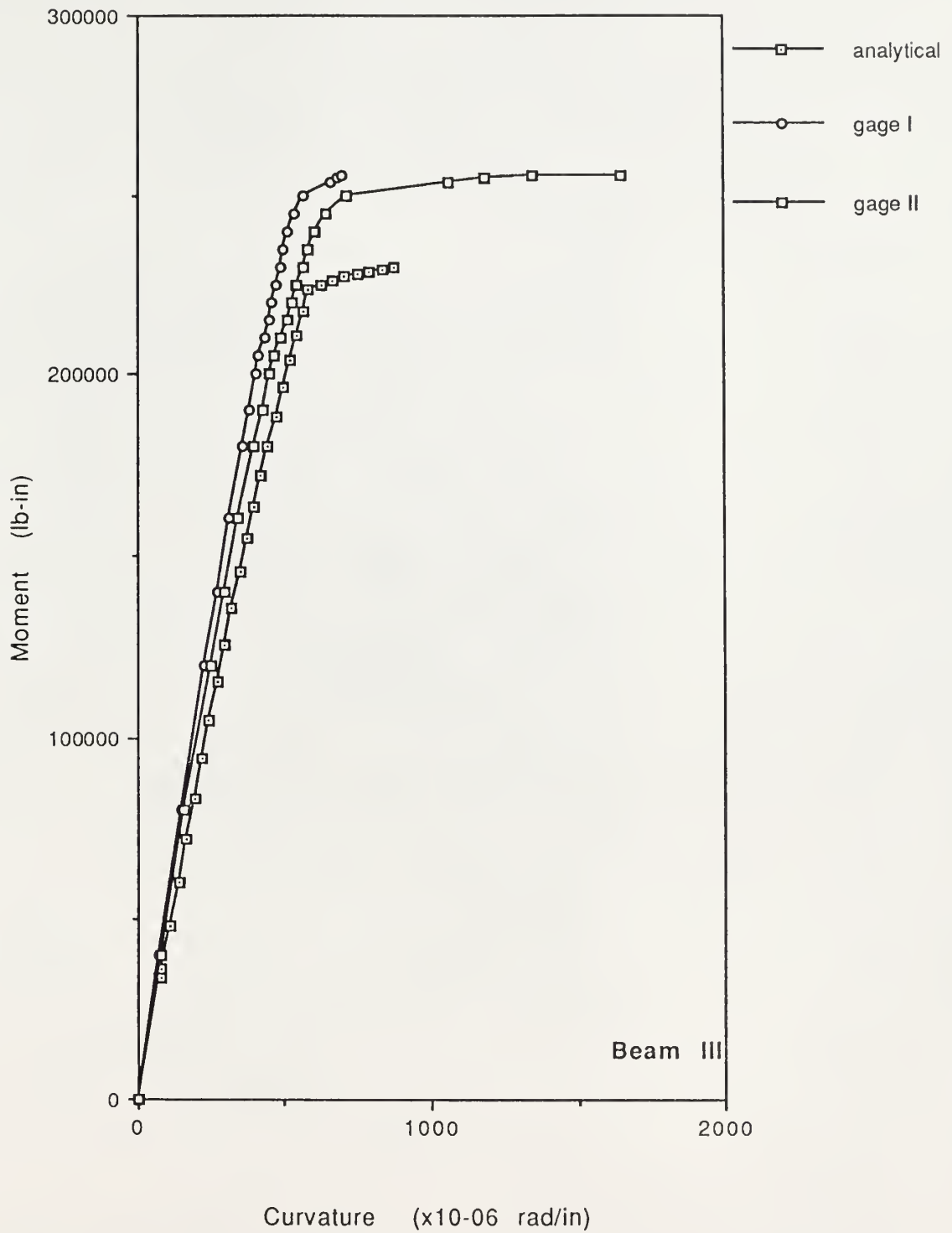Figure 5.15: Moment Curvature Relationship for Beam II.

Figure 5.16: Moment Curvature Relationship for Beam III.

5.5   SUMMARY OF RESULTS

The results from the different types of analysis conducted on the beams are summarized in Table VII. A schematic of the crack pattern observed in each beam is shown in Fig. 5.17.

In the elastic range, tensile cracking of the concrete occurs at a load of 1.5 to 2.0 times the predicted values. All three beams exhibit elastic behaviour far beyond what is predicted. Moment-Curvature relationships also show a far greater stiffness in the beams than the predicted stiffness. Service loads obtained from the AISC Working Stress Analysis are well within the total loads at which the beams show elastic behaviour.

In the ultimate range, results obtained from the ACI Ultimate Load Analysis are found to be very conservative in comparison to the test results. Since the beams were designed on the basis of ultimate moments, considering a strength factor of 0.9, these results appear to be much lower than the corresponding experimental results. But, even after providing an allowance of 10 % to the calculated moments for all the beams, the difference between the experimental and analytical values are substantial, on an average approximately 32 % , with respect to the analytical values.

From the moment curvature analysis, which is generally more accurate, an average increase of about 17 % with respect to the analytical values is observed. An interpretation for the greater stiffness and strength of the beams may be attributed to the general stiffness of the arrangement of reinforcement, and to a certain extent, a contribution from the shear strength of the beam to flexure.
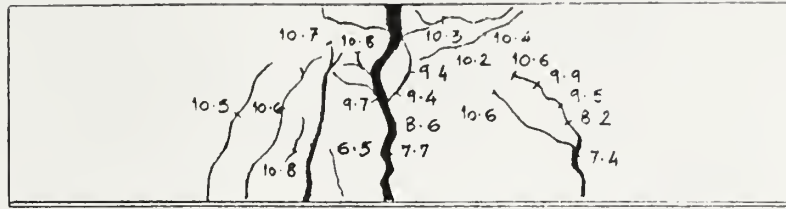
Beam I
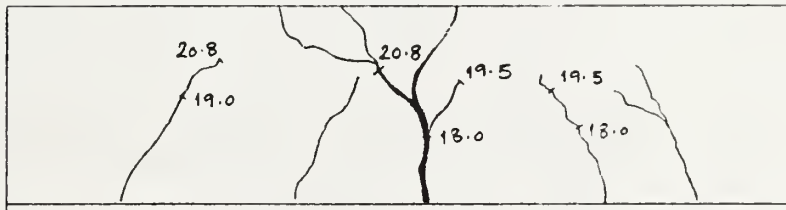
Beam II
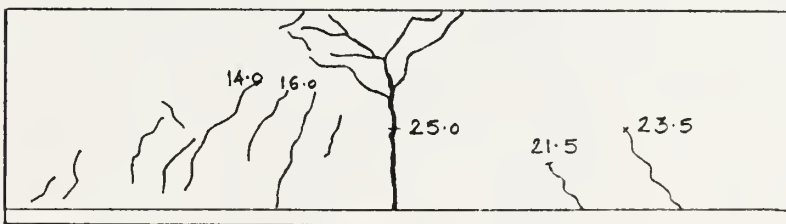
Beam III

Note: Value mentioned alongside crack is the total applied load

Figure 5.17: Crack Pattern in the Beams.

Chapter 6

SUMMARY

6.1   SUMMARY

The purpose of this investigation was to study the overall flexural behaviour of beams reinforced with plates to serve as tensile reinforcement in concrete beams. Three beams with different plate thickness were constructed and tested until failure. Experimental results were compared with results from an ultimate load and moment curvature analysis.

The overall flexural behaviour of the beams was found to be satisfactory. The beams showed greater stiffness and strength as compared to results observed from a moment curvature and ultimate load analysis.

6.2   RECOMMENDATIONS FOR FURTHER STUDY

This research covered a preliminary investigation of the proposed scheme of reinforcement in concrete beams by studying the overall flexural behaviour of simply supported beams.

An expanded experimental program for the study of the following is recommended :

1. Study of the horizontal slip behaviour by noting actual slip at the steel-concrete interface and determining the ultimate capacity of the shear connectors from push-out tests.

2. Study of the beams in vertical shear by constructing specimens with varying shear spans.

3. Comparing results with companion beam specimens made of conventionally reinforced concrete.

4. Construction of two span continous beam specimens to study flexural behaviour in the negative moment region.

APPENDIX-A

DESIGN DETAILS FOR BEAM III (OLD)

(A) Design for flexure.

$D = 6.5''$	$f_y = 36$ ksi
$t = 0.375''$	$f'_c = 4000$ psi
$b = 3.0''$	$\beta_1 = 0.85$
$d = 6.3125''$	

1. Balanced Steel Ratio (ρ_b):

$\frac{c}{d} = \frac{0.003}{\frac{36}{29 \times 10^6}+0.003} = 0.7073$

$K = 0.85 f'_c \beta_1 = 0.85 \times 4000 \times 0.85 = 2890$

$\rho_b = \frac{K}{f_y} \cdot \frac{c}{d} = \frac{2890}{36000} \times 0.7073 = 0.0568$

2. Steel Reinforcing Ratio (ρ):

$\rho = \frac{t}{d} = \frac{0.375}{6.3125} = 0.0594$

$k = \frac{\rho}{\rho_b} = 1.046$

3. Moment Capacity of the Beam (M_u) :

$M_u = \phi \rho f_y b d^2 (1 - \frac{0.59 \rho f_y}{f'_c}) = 157.5$ in-kips.

(B) Design for Shear.

Vertical Shear

1. Ultimate Shear Load Acting on the Beam (V_u):

$V_u = P_u = \frac{M_u}{20} = 7.86$ kips

2. Shear to be carried by the stirrups (V_s):

$V_c = 2\sqrt{f'_c} bd = 2.4$ kips.

$V_s = \frac{V_u}{\phi} - V_c = 6.85$ kips.

3. Stirrup Spacing (s_v):

Minimum value from

$$s_v = \frac{A_v f_y d}{V_s} = \frac{0.11 \times 40 \times 6.3125}{6.85} = 4.04''$$

or $s_v = d/2 = 3.16'' \leftarrow$ controls

or $s_v = 24''$

Since V_s exceeds $4\sqrt{f_c'} bd$, stirrup spacing to be provided is $d/4 = 1.58'' \approx 1.5''$.

Horizontal Shear :

1. Horizontal Shear Force (V_h):

$V_h = \frac{A_s f_y}{2} = 20.25$ kips $\leftarrow$ controls

$V_h = \frac{0.85 f_c' A_c}{2} = 22.8$ kips

2. Stirrup spacing (s_h):

$n = \frac{V_h}{3.245} = 6.24 \approx 7$

$s_h = \frac{20}{7} = 2.85 \approx 2.5''$

(C) Final Stirrup Spacing :

$s_v = 1.5'' \leftarrow$ controls

$s_h = 2.5''$

From the point of view of welding the stirrups and considering the fact that the shear design provisions are conservative, spacing provided $= 2.0''$.

APPENDIX-B

```
C    PROGRAM TO DO A MOMENT CURVATURE ANALYSIS IN THE ELASTIC RANGE.

C    DEFINING THE VARIABLES
C    DEPTH            depth of the beam
C    TCK              thickness of the plate
C    ESTEEL           modulus of elasticity of the steel
C    FY               yield stress of the steel
C    C                depth of the neutral axis
C    EC               strain in concrete
C    ES               strain in the steel
C    TEN              tension force
C    COMP             compression force
C    AREA             area under stress curve in compression zone
C    YBAR             location of resultant from neutral axis
C    ARM              lever arm for moment
C    MOM              moment
C    CUR              curvature

C    DECLARING THE VARIABLES
     REAL MOM

C    CREATING FILES THAT ARE GOING TO BE USED
      OPEN (UNIT=10, FILE='PROJ.OUT')

C    INPUT SOME OF THE RELEVANT DATA
     WRITE (*,*) 'INPUT THE DEPTH OF THE BEAM UNDER CONSIDERATION '
     READ (*,*) DEPTH
     WRITE (*,*) 'INPUT THE THICKNESS OF THE BEAM '
     READ (*,*) TCK
     WRITE (*,*) 'INPUT THE ELASTICITY OF THE STEEL '
     READ (*,*) ESTEEL
     WRITE (*,*)'INPUT THE YIELD STRESS OF THE STEEL '
     READ (*,*) FY

C    INITIALIZING THE VALUE FOR THE DEPTH OF THE NEUTRAL AXIS
     C = 2.0

C    MAIN BODY OF THE PROGRAM
      DO 300 EC = 100,3000,100

200       Y1 = -64.6
          Y2 = 4.83*EC/C
          Y3 = 9.04E-04*(EC/C)**2
          AREA = Y1*C + Y2*C*C/2.0 - Y3*C**3/3.0
          AREAY = Y1*C**2/2.0 + Y2*C**3/3.0 - Y3*C**4/4.0
          YBAR = AREAY/AREA
          COMP = AREA*3.0
          ES = EC*(DEPTH-C)/C
```

91

```
C    CHECK IF STEEL HAS YIELDED
          IF(ES.GE.FY/ESTEEL)THEN
              GOTO 400
          ENDIF

C    CALCULATE THE TENSION FORCE
          TEN = ES*ESTEEL*3.0*TCK

C    CHECK IF COMPRESSION AND TENSION FORCES ARE WITHIN A CERTAIN TOLERANCE
          IF (ABS(COMP-TEN).LE.25) THEN
              GO TO 100
          ENDIF

C    CHANGING THE POSITION OF THE NEUTRAL AXIS IF COMPRESSION AND TENSION
C    FORCES ARE UNEQUAL
          IF (COMP.GT.TEN) THEN
              C = C - .001
              GO TO 200
          ELSE
              C = C + .001
              GO TO 200
          ENDIF

C    CALCULATE THE MOMENT AND CURVATURES
100      ARM = (DEPTH-C) + YBAR
          MOM = (COMP+TEN)/2.0*ARM
          CUR = EC/C
           WRITE (10,*) 'EC','ES','MOM','CUR'
          WRITE (10,*) EC,ES,MOM,CUR

300   CONTINUE

400   STOP
       END
```

92

```
C    PROGRAM TO DO A MOMENT CURVATURE ANALYSIS IN THE INELASTIC RANGE.

C    DEFINING THE VARIABLES
C    DEPTH           depth of the beam
C    TCK             thickness of the plate
C    ESTEEL          modulus of elasticity of the steel
C    FY              yield stress of the steel
C    C               depth of the neutral axis
C    EC              strain in concrete
C    ES              strain in the steel
C    ECS             starting strain for concrete for this analysis
C    TEN             tension force
C    COMP            compression force
C    AREA            area under stress curve in compression zone
C    YBAR            location of resultant from neutral axis
C    ARM             lever arm for moment
C    MOM             moment
C    CUR             curvature

C    DECLARING THE VARIABLES
     REAL MOM

C    CREATING FILES THAT ARE GOING TO BE USED
     OPEN (UNIT=10, FILE='PRON.OUT')

C    INPUT OF SOME OF THE RELEVANT DATA
     WRITE (*,*) 'INPUT THE DEPTH OF THE BEAM UNDER CONSIDERATION '
     READ (*,*) DEPTH
     WRITE (*,*) 'INPUT THE THICKNESS OF THE BEAM '
     READ (*,*) TCK
     WRITE (*,*) 'INPUT THE ELASTICITY OF THE STEEL '
     READ (*,*) ESTEEL
     WRITE (*,*)'INPUT THE YIELD STRESS OF THE STEEL '
     READ (*,*) FY
     WRITE (*,*)'INPUT THE VALUE FOR THE STARTING STRAIN IN CONCRETE'
     READ (*,*) ECS

C    INITIALIZING THE DEPTH OF THE NEUTRAL AXIS
     C = 2.0

C    MAIN BODY OF THE PROGRAM
     DO 300 EC = ECS,3000,100

200      Y1 = -64.6
         Y2 = 4.83*EC/C
         Y3 = 9.04E-04*(EC/C)**2
         AREA = Y1*C + Y2*C*C/2.0 - Y3*C**3/3.0
         AREAY = Y1*C**2/2.0 + Y2*C**3/3.0 - Y3*C**4/4.0
         YBAR = AREAY/AREA
```

```
                COMP = AREA*3.0
                TEN = FY*3.0*TCK

C    CHECK IF COMPRESSION AND TENSION FORCES ARE WITHIN A CERTAIN TOLERANCE
            IF (ABS(COMP-TEN).LE.25) THEN
                GO TO 100
            ENDIF

C    CHANGING THE DEPTH OF THE NEUTRAL AXIS IF COMPRESSION AND TENSION
C    FORCES ARE UNEQUAL
            IF (COMP.GT.TEN) THEN
                C = C - .001
                GO TO 200
            ELSE
                C = C + .001
                GO TO 200
            ENDIF

C    CALCULATE THE MOMENTS AND CURVATURES
100         ARM = (DEPTH-C) + YBAR
            MOM = (COMP+TEN)/2.0*ARM
            CUR = EC/C
            ES = EC*(DEPTH-C)/C
             WRITE (10,*) 'EC','ES','MOM','CUR'
            WRITE (10,*) EC,ES,MOM,CUR

300  CONTINUE

            STOP
            END
```

ACKNOWLEDGEMENTS

Bibliography

[1] "Tentative Recommendations for the Design of Composite Beams and Girders for Buidings," Joint ASCE-ACI Committee on Composite Construction, *Journal of the Structural Division*, ASCE, Vol. 86, No. ST12, Proc. Paper 2692, December, 1960, pp. 73-92.

[2] Salmon, Charles. G. and Wang, C.K., "Steel Structures-Design and Behaviour," Second Edition, Harper & Row, 1980, pp. 917-967.

[3] Iyengar, H.S., "State-of-the-Art Report on Composite or Mixed Steel-Concrete Construction for Buildings," For the Structural Specification Liaison Committee, American Society of Civil Engineers, 1977.

[4] Holloway, R.T., "Precast Composite Sections in Structures," *Journal*, American Concrete Institute, Vol. 69, No. 2, February 1972, pp. 85-93.

[5] Snow, F., "Formwork for Modern Structures," Chapman and Hall, London, 1965, 128 pp.

[6] Gogoi, S., "Interaction Phenomenon in Composite Beams and Plates," Thesis submitted to the Imperial College of Science and Technology, University of London, in 1964, in partial fulfillment of the requirements for the degree of Doctor of Philosophy.

[7] Johnson, R. P., "Research on Composite Steel-Concrete Beams, 1960-1968," *Journal of the Structural Division*, ASCE, Vol. 96, No. ST3, Proc. Paper 7122, March 1970, pp. 445-459.

[8] Viest, Ivan M., Chairman, "Composite Steel-Concrete Construction," Report of the Subcommittee on the State-of-the-Art Survey of the Task Committee on Composite Construction of the Committee on Metals of the Structural Division, *Journal of the Structural Division*, ASCE, Vol. 100, No. ST5, May 1974, pp. 1085-1139.

[9] Viest, Ivan M., "Review of Research on Composite Steel-Concrete Beams," *Journal of the Structural Division*, ASCE, Vol. 86, No. ST6, June 1960, pp. 1-21.

[10] Chapman, J.C., "Composite Construction in Steel and Concrete- The Behaviour of Composite Beams," *The Structural Engineer*, Vol. 42, No. 4, April 1964, pp. 115-125.

[11] Daniels, J.H., "Recent Research on Composite Beams for Bridges and Buildings," *Civil Engineering Transactions*, The Institution of Engineers, Australia, Vol. CE14, No. 2, October 1972, pp. 228-233.

[12] "Report on Composite Construction in Structural Steel and Concrete," Institution of Structural Engineers, London, 1964.

[13] Cassillas, J. G.de L., Khachaturian, N and Siess, C.P., "Studies of Reinforced Concrete Beams and Slabs Reinforced with Steel Plates," Civil Engineering Studies, *Structural Research Series No. 134*, University of Illinois, 1957.

[14] Teraszkiewicz, J.S., "Static and Fatigue Behaviour of Simply-Supported and Continuous Composite Beams of Steel and Concrete," thesis submitted to Imperial College, London, in 1967, in partial fulfillment of the requirements for degree of Doctor of Philosophy.

[15] Perry, E. S., "A Study of Dynamically Loaded Composite Members," thesis submitted to the University of Texas at Austin, in 1964, in partial fulfillment of the requirements for the degree Doctor of Philosophy.

[16] Perry, E. S., Burns, Ned H., and Thompson Neils J., "Behaviour of Concrete Beams Reinforced with Steel Plates Subjected to Dynamic Loads," *Journal of the American Concrete Institute*, Vol. 64, No. 10, October 1967, pp. 662-668.

[17] Fauchart, J. and Sfintesco, D., "The Development and Use of the Robinson Composite Deck in France", *Reports of the Working Commissions, Symposium on Wearing Surfaces for Steel Bridge Decks*, International Association for Bridge and Structural Engineering, 1968, pp. 155-165.

[18] "New Alma Bridge over the Seine in Paris," Acier-Stahl-Steel, No. 3, March 1973, pp. 120-127.

[19] "The Paris-Massena Bridge, A Cable-Stayed Structure," Acier-Stahl-Steel, No. 6, June 1970, pp. 278-284.

[20] ACI Standard 318-83, "*Building Code Requirements for Reinforced Concrete (ACI 318-83)*," American Concrete Institute, Detroit, 1983.

[21] Winter, George and Nilson Arthur, "Design of Concrete Structures," McGraw Hill Publications, 10 ed., 1986.

[22] AISC, "*Manual of Steel Construction*", 8th ed., Chicago, 1980.

[23] "Shear and Diagonal Tension," Pt.2 Report of ACI-ASCE Committee 326, *J.ACI*, vol.59, pp. 277, 1962 (with extensive bibliography).

[24] Slutter, Roger G. and Driscoll, George. C., "Flexural Strength of Steel-Concrete Composite Beams," *Journal of the Structural Division* , ASCE, 91,ST2, April 1965, pp.71-99.

[25] Mattock, A.H., Kriz, L.B. and Hognestad, E., "Rectangular Concrete Stress Distribution in Ultimate Strength Design," *Journal of ACI*, Vol. 57, pp. 875, February 1961.

[26] Dudley, C.K. and Park R., "Flexural Members with Confined Concrete," Proceedings ASCE, *Journal of the Structural Division*, Vol. 97, No. ST7, pp. 1969-1990, July 1971.

[27] Carrasquillo, R.L., Slate, F.O. and Nilson, A.H., "Properties of High Strength Concrete Subject to Short-Term Loads," *J.ACI*, Proc., Vol. 78, No. 32, pp.179-186, 1981.

STUDY OF THE FLEXURAL BEHAVIOUR OF CONCRETE BEAMS REINFORCED WITH STEEL PLATES

By

ASIT N. BAXI

B.E., M. S. University of Baroda, India, 1986

———

AN ABSTRACT OF A MASTER'S THESIS

Submitted in partial fulfillment of the
requirements for the degree

MASTER OF SCIENCE

Department of Civil Engineering

KANSAS STATE UNIVERSITY
Manhattan, Kansas
1989

Abstract

The purpose of this investigation was to examine the flexural behaviour of an alternative method of reinforcing concrete beams. Longitudinal steel reinforcing bars of a conventionally reinforced concrete beam are replaced by mild steel plates. Vertical stirrups are replaced by vertical steel reinforcing bars welded to the plate. The entire assembly is easy to prefabricate and is placed directly in the joist form. After casting of the concrete and stripping of the forms, the steel plate, exposed on the underside of the joist, can be used to support mechanical and electrical equipment, suspended ceilings and interior partitions.

A series of three beams, with varying steel reinforcing ratios, was tested in four point bending until failure. Load-strain and load-deflection data and cracking patterns were noted. Results from the experiments were compared with results from various analyses in the elastic and ultimate range.

The overall flexural behaviour of the beams was found to be satisfactory. The beams showed greater stiffness and strength as compared to results observed from the moment curvature and ultimate load analysis conducted in the ultimate range.